Master Thesis

Comparison of Disparity Algorithms for Stereoscopic Video

Ben John

May 2016

Supervisor: Dr. Stephan Kopf

Department of Computer Science IV
Prof. Dr.-Ing. W. Effelsberg

School of Business Informatics and Mathematics
University of Mannheim

Abstract

Stereoskopische Videos speichern zwei separate Ansichten einer Szene, die sich üblicherweise nur in geringen horizontalen Verschiebungen der Pixel unterscheiden. Diese Pixelverschiebungen (Disparity) resultieren aus den unterschiedlichen Entfernungen der Objekte in der Szene. Ziel der Master-Abschlussarbeit ist es, bestehende Verfahren zur Berechnung der Disparity zu analysieren, geeignete Verfahren für Videos auszuwählen und diese zu implementieren. Ein spezieller Fokus soll auf Erweiterungen für Videos liegen, indem beispielsweise vorherige oder zukünftige Frames berücksichtigt werden. Zur Messung der Qualität der implementierten Verfahren sollen bestehende stereoskopische Bild- und Videoarchive genutzt werden.

Contents

List of Figures

List of Tables

1 Introduction

1.1 Motivation

Obtaining depth information as additional data to infer intents from human gestures has arrived in mainstream computing with the release of Kinect at November 4th, 2010[1]. Kinect is a hardware add-on for the Xbox video gaming console which enables users to interact visually with the console without actually using a controller or any other peripheral. The Kinect utilizes two cameras, one capturing colored and the other monochrome images. The monochrome sensor is used in combination with an infrared laser projector to obtain depth information via time of flight (TOF). Time of flight is a method to measure the time light needs to reach objects and then calculate the distance.

With deducing intents from human gestures a step in the field of artificial intelligence was made as the computer is now able to interpret human body language. As this means processing an enormous stream of data (gathering and processing frame by frame) it represents a dataset of large and complex nature, also known as big data. This also implies the need for new data processing techniques in comparison with traditional ones. As a result one could say that computer vision is linked to both, artificial intelligence and big data. New applications which arose from the combination of those topics are for instance:

- robotic,
- medical image analysis,
- automatic surgery,
- 3DTV,
- video compression,
- autonomous driving.

[1] `http://gizmodo.com/5563148/microsoft-xbox-360-kinect-launches-november-4`

Besides the technology of time of flight laser sensors - such as the Kinect[2] - there exists also the possibility to obtain depth information from stereo images by analyzing coherent images with so called disparity algorithms. Thus, it is sufficient to have two calibrated aligned cameras (a stereo camera) to acquire disparity information and calculate the depth at each point. But this leads to another fundamental problem of stereo matching: stereo correspondence, that basically means the labelling of pixels, i.e. which pixel of the left image belongs to the corresponding pixel on the right image as projection of the same three-dimensional point from the captured world projected to the image plane in every image. This problem of stereo correspondence has to be solved in order to actually match those and calculate the disparity. According to Scharstein and Szeliski, stereo correspondence is one of the most heavily investigated topics in computer vision [40]. As there is still a lot of research going on, no algorithm is working without any mistakes and also the runtime is a bit quirky, Microsoft Kinect established itself as a real alternative. This leads us to one of the disadvantages of Kinect sensor: Kinect is sensitive to other infrared sources (like sunlight) due to its nature of utilizing an infrared laser projector to acquire depth information, a stereo camera does not have this issue. Although using two coherent images also have some disadvantages which will be discussed later on, it is an alternative way to receive depth information. Especially thinking about autonomous driving during which at day a lot of sunlight is involved in, other techniques to estimate how far an object is away from one another are necessary to ensure a certain accuracy and fault-tolerance.

Although the topic of this thesis is neither about artificial intelligence nor big data the foundations and algorithms discussed can help machines to sense their environment through cameras, identify objects and estimate the distances towards each other. With the support of neuronal networks computers may also deduce intents, reason about their environment and then execute defined actions. In conclusion computer vision is a research field on its own but other fields may also benefit from the results. Computer vision establishes itself on the consumer market as more research is done. The upcoming iPhone supports this as it will feature a dual camera system [3]. In the year 2011 LG and HTC released the LG Optimus 3D[4] and corresponding the HTC Evo 3D[5]. Both had a stereo camera implemented and an auto-stereoscopic display attached. This enables one to view photos or videos taken in stereographic 3D without the actual need for additional peripheral

[2] Besides the consumer market, for autonomous driving or robotic research Velodyne is a well-known sensor.

[3] `http://9to5mac.com/2016/02/03/sony-dual-cameras-iphone-7-plus/`, 2016-02-22.

[4] `https://en.wikipedia.org/wiki/LG_Optimus_3D`

[5] `https://en.wikipedia.org/wiki/HTC_Evo_3D`

like 3D glasses. Both can be seen as an experiment as there was no big distribution, Apple normally focuses on the mainstream consumer market, opening up the box of possibilities and the need for such algorithms even further. One example application for such a consumer-driven market could be the reconstruction of a face after taking a photo. There exist no method to reconstruct a whole 3D model without having stereo images from all angles of the face, but it is possible to trick the user in having captured a 3D photo. Another concrete example for an application regarding depth estimation in stereo videos: detecting moving people in a stereo video and calculate the distance to the camera of each person[6].

1.2 Assignment

The usage and applications of computer vision are huge as seen in the motivational introduction. For understanding how disparity algorithms work it is important to have knowledge of various topics in computer vision. Therefore it was difficult to decide what should be in the thesis and what can be left out. The thesis' main goal is to provide an overview of selected disparity algorithms for stereoscopic videos and evaluated those. Scharstein and Szeliski justified their tiny selection of disparity algorithms with the following: "Compiling a complete survey of existing stereo methods [...] would be a formidable task, as a large number of new methods are published every year." [40]. That said the ones with well documented source code and a research paper, also adaptable within the time scope of this thesis, were integrated.

- The thesis should provide a good fundamental knowledge base for an advanced insight into the area of disparity algorithms for stereoscopic images and videos.
- Existing datasets are examined. Additionally, a novel dataset from the Lehrstuhl für Praktische Informatik IV[7] is presented.
- Based on existing paper and source code, different state of the art algorithms are analyzed and evaluated.
- As there exist a lot of different unaligned code for evaluating / comparing images the decision towards a new implementation of an evaluation suite with OpenCV was made.

[6] http://de.mathworks.com/help/vision/examples/depth-estimation-from-stereo-video.html
[7] http://ls.fmi.uni-mannheim.de/de/pi4/

- An idea of smoothing the computed disparity maps over time is presented. The smoothing should reduce occurring noise.
- Moreover quality metrics for evaluating those algorithms are defined.
- The algorithms are evaluated on different datasets. The runtime is also measured.
- As a benefit the results can be analyzed visually via a web front-end.
- Finally the results are discussed and future outlook is given.

1.3 Outline

The main purpose of chapter 2 is to give an overview of terms and techniques used in this thesis. The following chapter 3 focuses more on disparity algorithms and related work. To give an overview of state of the art algorithms a small summary of current used disparity algorithms is made. This will create the foundations for the later implementation. Chapter 4 describes the implementation and explains reasons for building an evaluation engine. The details of the implementation are explained afterwards. In addition the integration of existing algorithms is illustrated. The evaluation engine was fed with datasets which are introduced in chapter 5. This chapter also explains the used quality metrics and describes the resulting outcome accurately. In the end the results of this thesis are reflected in the concluding chapter. Besides some future work, split in low- and high-level, is pointed out.

2 Foundations

In this chapter the foundations for related work and the implementation are built. As a first step, computer vision is introduced with a short explanation how image representation works from a computer's perspective. Human visual perception is put in contrast to how computers perceive and interpret their environment. In addition, the labelling problem regarding stereo correspondence and the disparity between stereo images is illustrated. Furthermore, the depth calculation as well as the taxonomy of disparity algorithms is depicted. Finally, optical flow, a technical method that measures direction and movement of every pixel based on dominant movement in the original scene, is introduced to round this chapter up.

2.1 Computer vision

Computer graphics describes the terms and definitions of everything which has to do with basically treating images programmatically on a computer, interpreting and working with them. To give an example, the applications of computer graphics range from image representation, image creation, image transformations to applications of color models. Computer vision shares concepts from the domain of computer graphics, but works in reverse. Instead of modeling a scene and generating an image of it, computer vision optically measures the real world and tries to analyze it by applying models to the captured images. For instance, typical jobs are to get information out of an image, like image segmentation, edge detection, classification, and feature[1] point detection.

A simple example would be to imagine a face of a human being captured by a camera, which may produce errors due to lens distortion, shaky capturing, and sampling of the chip. Image editing would be useful to optimize the image by correction of contrast or brightness, cropping, or further adjustments. The tasks of computer vision are more in analyzing and understanding images for instance (just to name a few):

[1] Geometric shapes or more complex classifiers that are clearly recognizable.

- face localization to know the areas of faces on images,
- feature matching to detect the face on other images,
- feature tracking to track the movement of a person, or
- 3D reconstruction of a facial model.

Image representation

Two different methods exit of handling images on a computer. On the one hand, a vector image describes its content by representing forms like a circle, line, curve, or rectangle. The properties of these forms and shapes are also included, for instance, coloring, size, and origin. So a vector image basically contains those forms and shapes, their properties and a description of how they are all composed together.

On the other hand, it may become pretty complex using vector images to represent the real-world. In contrast to those there also exist raster images. Raster images (sometimes the term bitmap images is used) are a form to represent natural images, e.g. captured by a CCD[2] image sensor from a digicam. Capturing means sampling information on a matrix of light sensitive sensors to transform received signals into a matrix of color values of the same size.

Both types of images use a coordinate system to describe either the placement of elements (like written above with the properties size and origin of each element) or to describe how each point looks like. The coordinate system most widely used working with images starts in the upper left at the point $(0, 0)$, with the x-axis extending to the right and y-axis extending to the bottom. This can be seen as a grid system with the size of the image $width \times height$ representing $columns \times rows$. By describing how each point looks like the exact description of a pixel is meant [42].

One pixel in a grayscale image can range from $0 - 255$ describing the intensity of this pixel. 0 means black and 255 is fully white. In colored images a pixel can have more than one intensity value. More concrete, in a typical RGB[3] raster image each pixel contains three color channels, also called the RGB tuple. Thus

$$3 \cdot 1\ bytes = 3 \cdot 8\ bits = 3 \cdot 8 = 24\ bits$$

are stored per pixel utilizing RGB tuples. In C or C++ such pixel values are normally described as unsigned chars. A char represents eight bit and unsigned means

[2] CCD: charge-coupled device
[3] RGB: red-green-blue color channels

that it ranges from $0-255$ instead of -128 to 127. Sometimes RGB is used with an additional alpha channel specifying the degree of opacity, named RGBA[4]. The composition of these color channels orchestrate the final pixel value as it is obtained by, for example, an image sensor. Figure 2.1 depicts an example of a RGB raster image and shows the values of three pixels. The first marked pixel in figure 2.1 describes the RGB tuple with the following values $(237, 237, 237)$. Utilizing three color channels the final raster image then needs up to 24 bits per pixel, meaning an image the size $width = 300\ px$ and $height = 400\ px$ needs

$$300 \cdot 400 \cdot 24bits \cdot \frac{1\ byte}{8\ bits} = 360.000\ bytes$$

in memory. Images can be compressed with, for example, the JPEG algorithm but as the later implementation works only with pure raster images, as the unaltered values are examined, the amount of bytes as explained above is to be held in memory during the execution of the implementation.

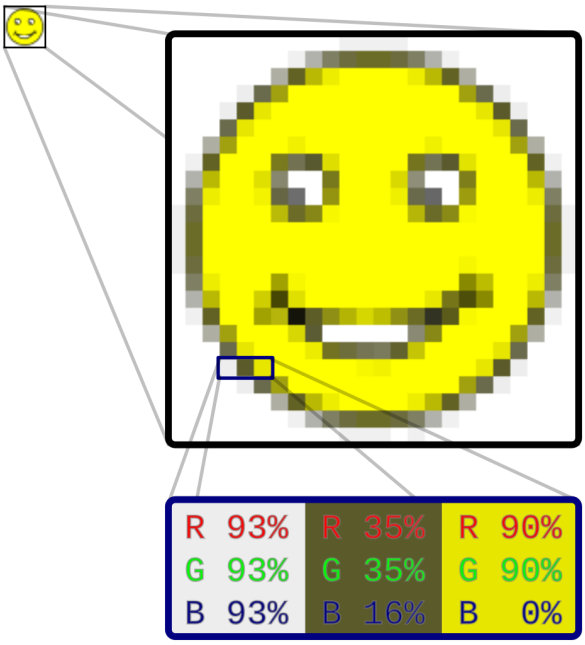

Figure 2.1: Example of a RGB raster image[5]

[4]RGBA: red-green-blue-alpha color channels
[5]Source (accessed 02/2016): `https://en.wikipedia.org`.

Human visual perception

In his manuscript 'Astronomia Pars Optica' from 1604, Kepler explains the use of both eyes for depth perception. He defined the term binocular as the composition of two latin words, 'bini' for double and 'oculus' for eye. With uniocular as 'uni' for one the sight with only one eye is meant. Binocular vision is then the vision creatures having two eyes obtain while using them together according to Kepler. According to Fahle [14] and Henson [18] creatures with binocular vision have several advantages over creatures with only uniocular vision. Not to mention all but three, the most important ones which affect the depth perception:

1. Considering human beings, the second eye increases the field of view [18]. About 120 degrees are the binocular field of view (projected on both eyes) and two uniocular fields of view with about 40 degrees.

2. This also leads to another advantage with occluded, half-occluded or non-occluded objects [14]. Looking at Figure 2.2, the point P is in focus of the human being. Something directly behind this point may be fully occluded by the object in point P. Most of the things besides are non-occluded. Something behind this point P may be half-occluded if it can be seen by either the left or the right eye.

3. An advantage of having two eyes is the third-dimension human beings perceive, which leads to the binocular disparity or retinal disparity. Both terms are used in the literature and both mean the same: extracting depth information out of two coherent retinal images (obtained by the human eyes) [11, 14].

Figure 2.2 depicts the mapping of the three points R, P and Q on the retina of each eye. The letter F stands for *foveae* in which the visual axis ends. The eye is constructed out of photoreceptor cells, mainly rods and cones. The rods are necessary for seeing at night while the cones are responsible for humans being able to see the world sharp. In the foveae is the peak of cones and it contains very few rods. This means that the human visual system works the way that the visual axis joins the point of fixation with the foveae. This can be seen in Figure 2.2 as the lines between F of each eye to the point of fixation P. Both eyes should be brought into convergence that the point of interest is projected onto the foveae of each eye. Everything on the horopter (the circle) is corresponding (e.g. P and Q), all points other than being on the horopter are non-corresponding (R) in terms of retinal disparity.

In the later described disparity algorithms which act like a tool for computers

to be able to see the shift of pixels from the left image to the right image, the human being does somehow the same. Humans experience the depth which is sensed unconsciously by the eyes and calculated by the brain in real-time. With two eyes basically two slightly different images are obtained. The brain acts as the computer which puts both coherent images together and extends the two-dimensional space into a three-dimensional space and calculates the position of the objects in the z-axis.

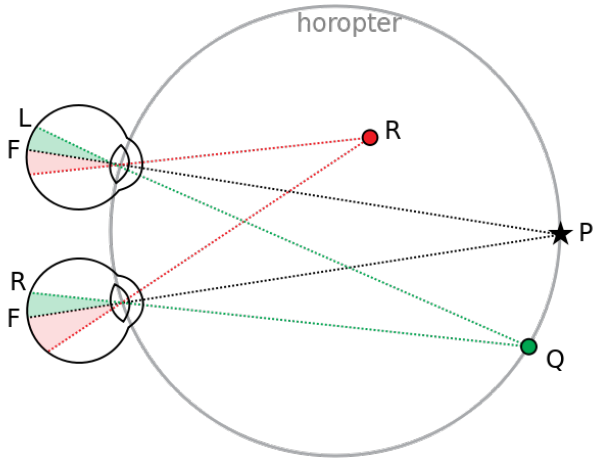

Figure 2.2: Binocular vision with horopter principle[6]

In contrast to the visual perception human beings perceive, computers need to do several steps to obtain disparity and calculate depth information:

- identify objects,
- identify layers,
- match objects / pixels in both images,
- calculate the shift of the pixels from left to right, and
- obtain final depth values.

The human brain enables human beings to see and experience the real-world three-dimensional. A computer has to be programmatically instructed to identify and group objects in both images [4, 11]. This is not an easy task as can be seen in the next sections.

[6]Source (accessed 02/2016): `https://en.wikipedia.org`.

Stereoscopy

To paint the bigger picture, stereoscopy and the illusion of depth are introduced. Stereoscopy is sometimes linked to the phrase 'the illusion of depth' as it is a technique used to add a third dimension to a flat image to simulate depth [4, 32]. Specifically, the goal is to show each eye a slightly different image and thus achieve depth perception in our brain. With so called stereoscope or special glasses depth perception can be transferred to the consumer in a cinema or at home via showing each eye a different image which then is composed to the final spatial perception.

There exist several techniques to create the stereoscopic effect. One of these glasses is the shutter system. The concept of a shutter glass is that it cycles a block (meaning only one eye is dispatched to the screen) with a certain frequency (usually about 120 fps[7], resulting in 60 fps per eye) synchronously with the 3DTV. This means that only one specific image is passed to exactly one of the consumers eyes. So each eye is shown about 60 fps which naturally is experienced as flicker-free. The older anaglyph 3D technique uses multiplied images tinted with red/cyan to filter out the respective image by the glasses filter foil, thus only one image is dispatched to one specific eye at a time. Nowadays the anaglyph 3D technique is sometimes used in magazines to show 3D graphics. As all techniques are not representing the real-world and the depth perception can be adjusted with for instance camera positioning (image one would reposition his eyes to perceive the real-world differently) they can be summarized as the illusion of depth.

Epipolar geometry

The geometry of stereo images, called epipolar geometry, plays an important role in understanding the mathematical equations in the upcoming section. The most important terms of epipolar geometry are:

- image plane,
- baseline,
- epipole,
- epipolar line, and
- epipolar plane.

[7] frames per second

The *image planes* in Figure 2.3 and Figure 2.4 are the blue surfaces which represent the captured image through the cameras O_L and O_R. The *baseline* is the line joining both camera centers with the image plane. Focusing on the figures, the baseline is the line going from O_L to O_R, as O reflects the origin (camera center). An *epipole* is the joint of the baseline with the image plane, referring to the symbols e_L and e_R. The *epipolar plane*, visualized as green triangle in Figures 2.3 and 2.4, is determined by point X and both origins O_L and O_R. It is the surface reflecting the z-axis, the depth. An *epipolar line* then is the intersection between the origin to the point of interest, in this particular case X, which lies on the epipolar plane and intersects the image plane.

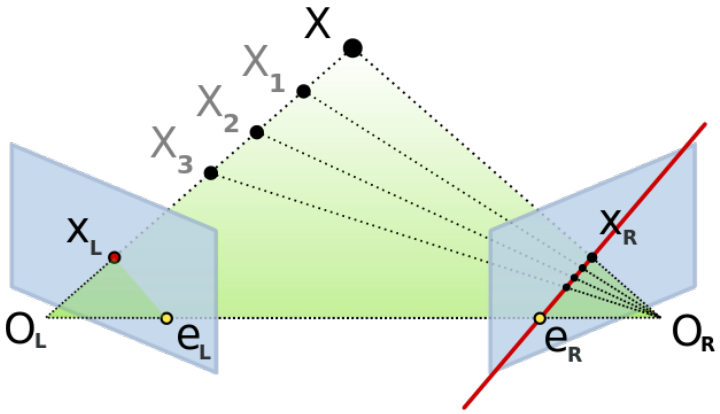

Figure 2.3: Epipolar geometry[8]

This results in an epipolar constraint [11]: Each image point X_i of a space point in the image plane, e.g. consider point X in Figure 2.3 must lie on the corresponding epipolar line $O_L\vec{X}$. More concrete focusing on Figure 2.3: this constraint states that the correspondence for a point on the epipolar line $O_L\vec{X}$ must lie on the line $e_r\vec{X}_r$. As seen above Figure 2.3 depicts the left and right view of an object in point X.

The Figures 2.3 and 2.4 both illustrate the epipolar geometry on a pair of unrectified images and the result after the rectification was done. Rectification[9] is necessary to reduce the search-space from two-dimensional to one-dimensional. For determining the exact position of X (possible positions X_i with $i = [1 \dots 3]$)

[8] Source (accessed 02/2016): `https://en.wikipedia.org`.

[9] Affine transformation (rotation and translation) neglecting geometric distortion to rectify the images.

the diagonal has to be scanned in the unrectified image. In the rectified image only the horizontal needs to be investigated. In the further proceeding this line is called the scanline which most of the algorithms operate on [9, 11]. After the rectification process the following two statements come true:

- Epipolar lines are parallel to the x-axis (horizontal).
- Corresponding points are on the same y-axis (vertical).

Implicitly the following two assumptions were made:

- the focal length f of both cameras which captured the images are the same,
- the origin of one camera is the so called camera principal point (the joint of the optical axis with the image plane and the fovea counterpart) [11].

In conclusion, corresponding points are constrained to be on the same line and thus depth can be inferred by using triangulation and camera parameters. Based on this, the investigations of stereo correspondence and the actual depth calculation using triangulation is discussed in more detail in the next sections.

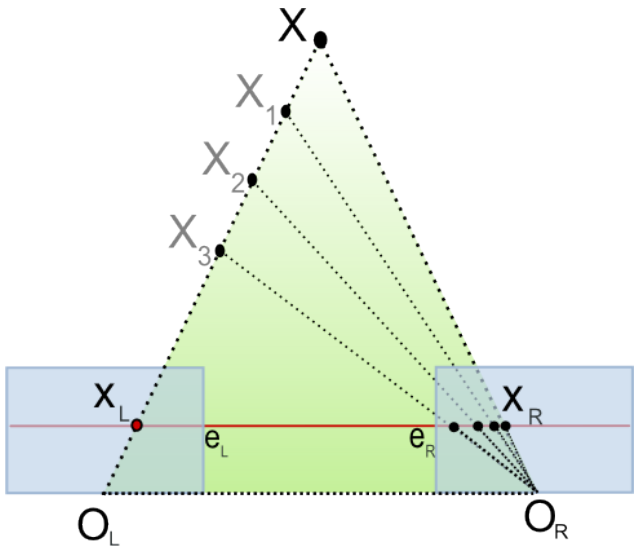

Figure 2.4: Epipolar geometry after image rectification[10]

[10]Source (accessed 02/2016): `https://en.wikipedia.org`.

2.2 Stereo correspondence

Stereo correspondence can be seen as a pixel labelling problem [11, 49] between two (or more) stereo images. The essential problem is to find corresponding pixels in images of different cameras and needs to be solved. Without knowing which points belong to each other in two separate stereo images, no conclusions can be drawn for instance calculating the disparity. Henceforth, while talking about images for stereo matching, rectified images are implicitly meant. If images are existing in an unrectified unaligned version then as a preprocessing step the images will be rectified.

Constraints

Stereo matching algorithms rely on several assumptions about the real-world. From the pioneer work of Marr and Poggio [33] the following constraints can be reasoned which are important for the development of such algorithms (also cf. [11, 26, 49]):

As a short remark: X_i is a point on a scanline in image i (i can be replaced with either L for left or R for right side) and thus only the x-position is mentioned.

Uniqueness
: As each pixel on a surface has one unique physical position in space, each pixel from each image has at most one disparity value.

Continuity
: The term smoothness constraint is also mentioned in the literature. Disparity can vary but smoothly almost everywhere in an image except at object boundaries which represent a discontinuity in depth, i.e. the difference of adjacent points should be small $||X_{L_1} - X_{R_1}| - |X_{L_2} - X_{R_2}|| < \varepsilon$.

Epipolar
: Recapture of the epipolar constraint from the section before: corresponding image points have to lie on the corresponding epipolar lines. If the epipolar lines are known to be parallel to the x-axis, the search space can be reduced to a 1D search space along the epipolar lines.

Ordering
: Following up the epipolar constraint: if the epipolar lines run in parallel to the x-axis, multiple consecutive image points have to lie on the same corresponding epipolar line in the same ordering.

Limit
: There is a defined disparity maximum (limit) d_{max} holding $|X_L - X_R| < d_{max}$, defining the maximum disparity value which can be found in a stereo image. Hence, $d(x, y)$ is in the range $[0 \dots d_{max} - 1]$.

Lambertian
: Algorithms for stereo matching also rely on the assumption of opaque lambertian surfaces, meaning a surface that reflects light equally into all directions and thus appears equally bright independent from where light is coming and where the camera is placed. Thus the algorithms can expect the intensities and colors of corresponding points to be almost the same.

Besides those constraints there also exist some common pitfalls which can disturb the result of algorithm.

Common pitfalls

Algorithms are using different metrics to analyze similarities in images along scanlines, in whole areas, or at a global view to then estimate the disparity. This can be challenging especially considering the upcoming traps. On the one hand, potential issues from the camera setup can be challenging, such as:

- photometric distortions,
- noise,
- calibration error of the cameras.

On the other hand, the scenery can be tricky:

- specularities and reflections,
- transparent objects,
- matching ambiguity,
- occlusions (missing data) and discontinuities.

These issues also challenge the algorithms to stereo match the pixels correctly. With matching ambiguities, constant or low-contrast regions are meant. A good example for that are textureless regions or repetitive structures. Textureless regions could contain a small set of matching pairs of pixels, other pixels of that region could be erroneously assumed the same. The presented constraints support the algorithms regarding those pitfalls.

Simplified stereo matching

Figure 2.5 depicts a simplified example of how stereo matching works on a one-dimensional search space: there exist two arrays with $length = 5$, one in the left and one in the right image. Assuming the top row $[p \dots t]$ reflects one row in the left image. The bottom row $[u \dots y]$ accordingly the same row in the right image. The pixel p, q, w and y are unmatched, e.g. occluded. Having a function $d(z)$ which returns the disparity for a given element z in those arrays, $d(r) = -2$ means the shift two to the left. Accordingly $d(s) = -2$ and $d(t) = -1$.

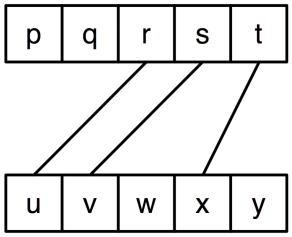

Figure 2.5: Two arrays illustrating stereo matching on a 1D search space [26].

Up to this point the epipolar geometry and the challenge with stereo matching were introduced. The upcoming section defines disparity, illustrates the disparity map, and the depth calculation.

2.3 Disparity map between stereo images

In the last two sections epipolar geometry and the problem with stereo correspondence were introduced. In this section the focus is on the term disparity, how disparity can be visualized via disparity maps, and how the depth can be calculated out of those disparity values.

Disparity

The disparity is the shift of a pixel / object (feature) between two or more images. An object may appear at position (x_1, y_1) in the left one and at position (x_2, y_2) in the right one. The disparity is the shift from the left position to the right one. With P_i declaring a point, left or right side, the following represents the disparity for two points in a two-dimensional space utilizing the pythagorean theorem:

$$D(P_L, P_R) = \sqrt{D_X^2(P_L, P_R) + D_Y^2(P_L, P_R)} \tag{2.1}$$

Henceforth, as the assumption of rectified images was made, only the horizontal disparity D_X is meant by the term 'disparity'.

$$D_X = |X_1 - X_2| \tag{2.2}$$

In other words, having a pixel (x_1, y_1) in a reference image (left) l and a pixel (x_2, y_2) in our matching image (right) r the correspondence is given by:

$$x_2 = x + |d(x_1, x_2)| \quad \text{with} \quad y_1 = y_2, \tag{2.3}$$

where $d(x, y)$ is the function which delivers values out of the disparity space (x, y, d) computed by the algorithms.

Resulting in matching pixels from one image to another, the disparity for each pixel-wise combination is calculated as seen in the previous subsection (simplified stereo matching) and presented here. Such disparities can also be seen as the inversed distances to observed objects. As a matter of fact, at the border of each image some pixels can not be calculated caused by the non-existing counterpart for matching. Those pixels with no fellow are called 'occluded' pixels. For example, in some cases pixels are hidden in one image by an object due to the blocking line of sight of this object.

Disparity map

In order to actually analyze the output of algorithms ground-truth data is necessary. An algorithm normally outputs a disparity map reflecting the disparity space (x, y, d). This disparity map can be seen as matrix having the size of the original image ($m \times n$) and containing values ranging from 0 to $d_{max} - 1$ utilizing one color channel (grayscale). The maximum disparity can be set via parameter for most of the algorithms and a feasible value which yields to sound results is 64. For better visual analysis the disparity maps are usually normalized to values ranging from $0 - 255$ [11, 34, 40]. Figure 2.6 c) shows the ground-truth data representing the disparity map. The disparity map depicts grayscale intensities with lighter gray representing pixels / objects closer to the camera.

Tying in with the term ground-truth Martull et al. created the first "highly realistic CG dataset that properly models real-world imperfections, while providing accurate ground truth." [34]. Without such datasets bad evaluation of stereo matching algorithms can be made as there would been no reference to evaluate against. Figure 2.6 shows the previous dataset of the University of Tsukuba, the well-known *Head and lamp scene*.

(a) left input image (b) right input image (c) ground-truth data

Figure 2.6: Tsukuba benchmark stereo image pair of the University of Tsukuba [34].

The input for a perfect algorithm would be the reference image (a) and the matching image (b). After computation the result would be similar to the ground-truth data (c). With evaluation metrics the computed disparity map is then compared to the ground-truth data. Measuring instruments serve as a quality indicator for an algorithm's performance. The above example is given for basic knowledge and understandability of how a disparity map actually looks like. Details of this process are examined in the evaluation Chapter 5.

Depth calculation

From an obtained disparity map and given camera parameters the depth can be calculated. The mathematical description of the following equations has been introduced by Cyganek and Siebert in Chapter 3.4.9 (Depth Resolution in Stereo Setups) of their book "*An introduction to 3D computer vision techniques and algorithms*" [11]. Assuming the focal length of the camera's lens and the baseline[11] are known, the following holds:

$$Z = \frac{f \cdot B}{d} \quad \text{and} \quad d = \frac{f \cdot B}{Z} \tag{2.4}$$

$$X = \frac{x \cdot Z}{f} \quad \text{and} \quad Y = \frac{y \cdot Z}{f} \tag{2.5}$$

where:

- Z is the distance along the z-axis (camera axis),
- f is the focal length,
- B is the baseline (in meters),

[11] The distance between both image sources.

- d is the disparity of the point.

After Z is determined, X and Y can be calculated using the usual projective camera equations (2.4-2.5) where the point (x, y) is the pixel location in the 2D reference image and (X, Y, Z) describes the real 3D position [4, 11, 34, 40]. Figure 2.7 depicts the depth calculation from disparity with X being the estimated point and $d = x - x'$.

The following subsection describes the more general steps of how disparity algorithms work, known as the taxonomy.

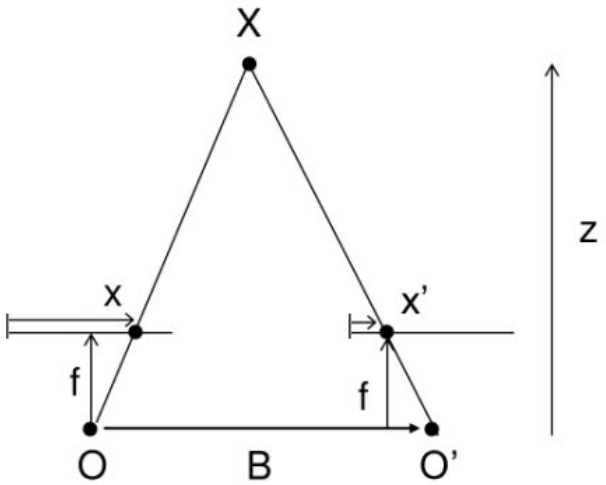

Figure 2.7: Depict of depth calculation from disparity.[12]

[12]Source (accessed 02/2016): `http://docs.opencv.org`.

2.4 Disparity algorithms

In the last sections different aspects affecting stereo matching were introduced. To get a better understandability of the algorithm's technique, this section focuses on the diversity and taxonomy of disparity algorithms.

Diversity of disparity algorithms

A lot of different algorithms exist and their workings differ slightly. According to Cyganek and Siebert [11], Scharstein and Szeliski [40], the following categories to separate disparity algorithms exist. Some of these classifications are discussed in more detail the related work Chapter 3.

First, the output of an algorithm is rated: they can create sparse or dense disparity maps. On the one hand, most of the algorithms produce a dense disparity map meaning that almost every pixel got a corresponding shift value. On the other hand, sparse algorithms only calculate values around, for instance, feature points (cf. feature matching). One advantage of sparse algorithms compared to dense disparity algorithms is that they are normally faster in computation but limited in applications. Approaches to interpolate sparse disparity maps into dense disparity maps exist, but they tend to produce inaccurate results in comparison to dense algorithms.

Second, Cyganek and Siebert [11] categorize direct and indirect methods. Indirect methods are feature based or operate in the transformed image space (cf. Chapter 6.3.7 in [11]). Direct methods use intensity based measures.

Finally, disparity algorithms are classified into local and global methods:

- Local Methods
  - Feature matching
  - Block (area) matching
- Global Methods
  - Belief propagation
  - Graph cuts
  - Dynamic programming
  - Layering (hierarchical scale-space)

Taxonomy of disparity algorithms

Assumptions need to be made before starting to describe the taxonomy of disparity algorithms:

1. The algorithm is fed with a pair of rectified images as input.
2. The algorithm produces a dense integer disparity map, which means that disparity is estimated at each pixel.
3. Most of the current algorithms works according to the following steps (see Figure 2.8)

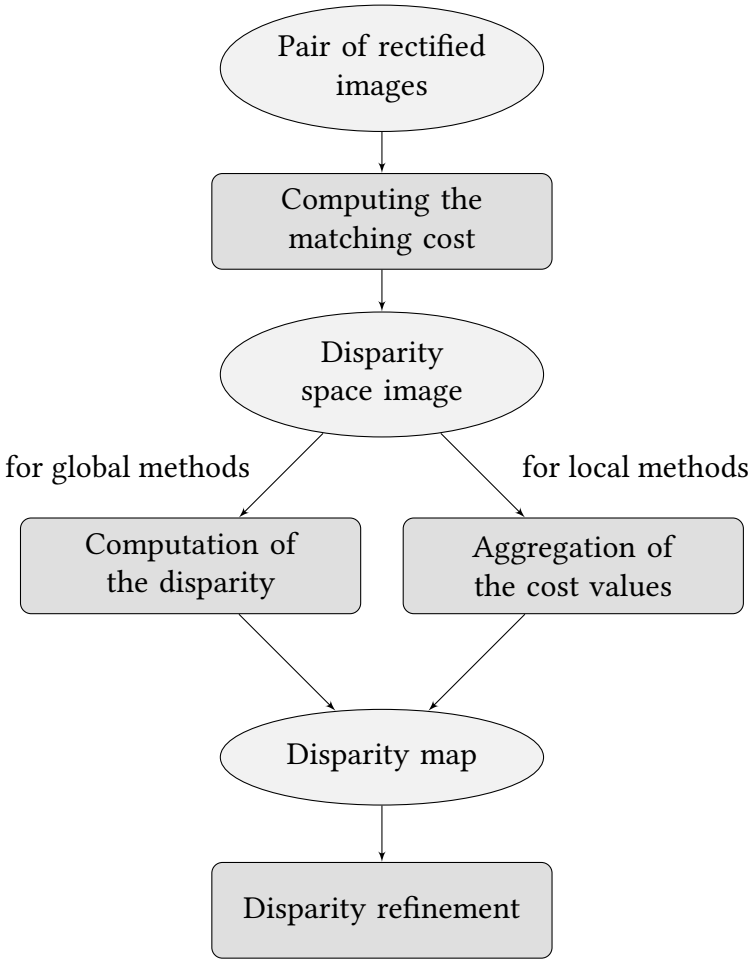

Figure 2.8: Basic processing flow of typical disparity algorithms [11, 40].

The upcoming subsections discuss the steps in more detail, especially regarding the computation of the matching cost and the subsequent aggregation.

Matching cost functions

At first, the similarities of pixels in both images are calculated. In general, the literature shows matching cost as the dissimilarities of pixels. The matching cost needs to be computed for the decision which pixel belongs to another. Hence, the cost needs to be low for similar pixels. Some of the matching criteria used for determining the matching cost are described in Table 2.1 cf. [7, 11, 17, 27, 40].

Method	**Formula**
Sum of absolute differences	$\sum_{i,j \in U} \lvert I_1(x_L + i, y_L + j) - I_2(x_R + i, y_R + j) \rvert$
Sum of squared differences	$\sum_{i,j \in U} (I_1(x_L + i, y_L + j) - I_2(x_R + i, y_R + j))^2$
Normalized cross-correlation	$\frac{1}{n} \sum_{x,y} \frac{(I_1(x_L, y_L) - \overline{I_1})(I_2(x_R, y_R) - \overline{I_2})}{\sigma_{I_1} \sigma_{I_2}}$

Table 2.1: Most common similarity measures

$I_k(x, y)$ stands for an intensity value of the image k at the point with given coordinates (x, y). The set $U = U(i, j)$ describes close-by points located around the point (i, j). The sum of absolute differences (SAD) similarity measure is one of the simplest ones and describes the difference between pixel values. The absolute intensity differences of both images I_1 and I_2 are summed up for all adjacent pixels in the neighborhood (described with U). Zero stands for the equality of both regions. In optimal images nearly every pixel in the left image should have a corresponding pixel in the right image, fulfilling the constraints from the section before, and thus the calculated SAD should sum up to zero. The lower the result, the more similar the pixels and the cheaper the matching cost are.

In the sum of squared differences (SSD) similarity measure the pixel differences are squared and summed up. This measurement needs a bit more computational power and is usually chosen to discriminate high differences. It can yield to better results if outliers need to be excluded and the difference is not strong enough while using SAD.

There also exist the normalized cross-correlation (NCC). Cross-correlation measures the correlation between two intensity values in a point (x, y). The normalized cross-correlation subtracts the mean $\overline{I}$ of the intensities and divides by the standard deviation σ_I to normalize the intensity values. This may be necessary to balance brightness variations. NCC is excluded in most scientific investigations regarding disparity algorithms as it behaves similar to SSD (cf. [11, 23, 40]).

Disparity space image

Related to the disparity space introduced in the section before, the disparity space image (DSI) should be defined. The DSI is an image or a function over a continuous or discretized version of the disparity space (x, y, d) and represents the matching cost (i.e. the dissimilarity) of a given $d(x, y)$. It can be imagined as a three-dimensional matrix with the x-axis meaning the column, the y-axis the disparity and each combination the matching cost for that particular value as the z-axis. The disparity space image $C(x, y, d)$ is the result of the matching cost values over all pixels and all disparities, where the function C that denotes the matching cost for the given input parameter. This leads to the aggregation step, during which the matching cost form the final disparity for local methods.

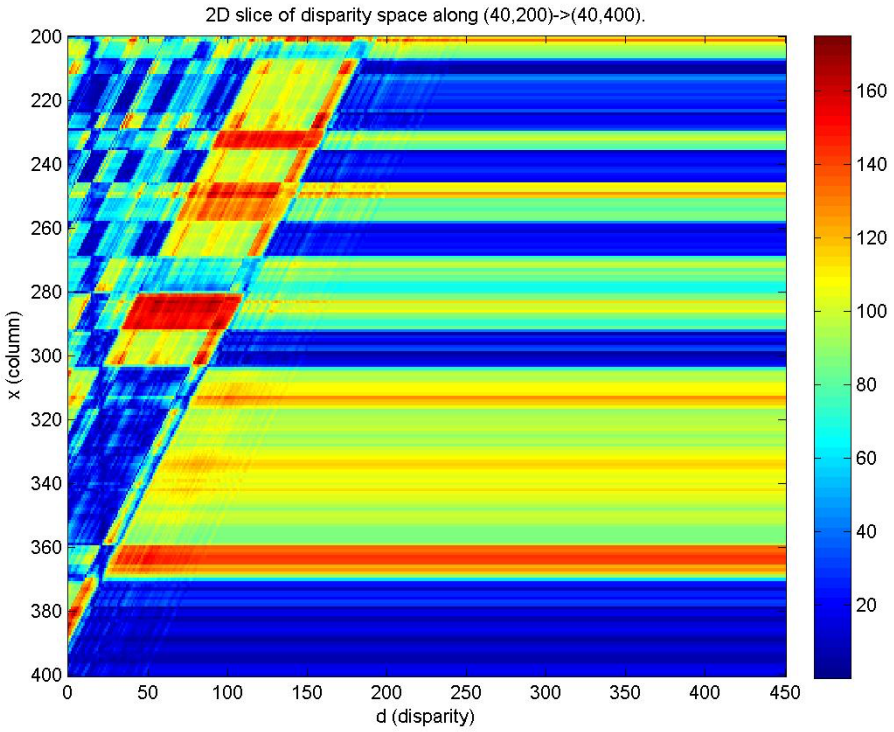

Figure 2.9: Illustration of a disparity space image.[13]

[13] Source (accessed 03/2016): `http://www.cs.virginia.edu/~cab6fh/CV_4/WRITEUP.html`.

Aggregation

In the aggregation step the decision has to be made, which discrete set of disparities represents the scene best [40]. As the matching cost values over all pixels and all disparities are stored in the DSI the minimum for each row is chosen as the best matching pixel and thus declared as the corresponding pixel. In other words: for every pixel the disparity with the lowest cost is selected. This strategy is known as the winner takes it all (WTA). [11, 40]. As the pixel with the lowest cost is chosen, the following holds:

$$d(x, y) = \arg\min_{d'} C(x, y, d'). \tag{2.6}$$

Disparity computation

After the aggregation, the actual disparity is computed in this step. It is split up for the two different methods: local and global.

(i) Local methods. Local methods focus on the matching cost computation and the cost aggregation steps. The final disparity computation is trivial as the minimum cost value (least dissimilarities) over each row is chosen (WTA).

(ii) Global methods. In contrast to local methods, global methods unify the three basic steps into a single one by defining an energy function to be minimized. It ties in with the labelling problem [44]. A row in the DSI can be imagined as the different labels (i.e. disparity values) one pixel can receive. The labelling problem describes the search of the disparity as the choice of the correct label. Each pixel should only have one label assigned in the end.

Let P be a set of pixels and D a set of disparities. The energy function aims to find a disparity d which minimizes some energy:

$$E(d) = E_{data}(d) + \lambda E_{smooth}(d). \tag{2.7}$$

The data term $E_{data}(d)$ defines the matching cost for a given disparity function d and expresses how well the disparity function d matches with the input image pair. C is the matching cost DSI:

$$E_{data}(d) = \sum_{(x,y)} C(x, y, d(x, y)). \tag{2.8}$$

As each pixel should be matched to a good find in the other image but simultaneously the adjacent pixels should be normally piecewise smooth, i.e. about the

same value / intensity, the smoothness term $E_{smooth}(d)$ is introduced to reflect that (cf. stereo correspondence constraints). The λ is introduced to control how much the smoothness term should influence the overall data term. To make the smoothness term computationally affordable it is, depending on the algorithm, usually restricted on the differences between adjacent pixel disparities [11, 40], i.e. the disparity gradient:

$$E_{smooth}(d) = \sum_{(x,y)} p(d(x,y) - d(x+1,y)) + p(d(x,y) - d(x,y+1)), \quad (2.9)$$

where p is a "monotonically increasing function of disparity difference" [40]. Depending on the used algorithm, other smoothness term functions exist. The optimization problem to solve is defined as the minimization of the energy function, i.e.:

$$D = \arg\min_{d} E(d), \quad (2.10)$$

where D is the disparity map containing the final values for every (x, y) and d a set of parameters or a disparity function affecting the energy value.

The search space for finding a solution is large, as an $n \times m$ image with k disparities has about $k^{n \times m}$ possible solutions. According to Scharstein and Szeliski [40], Cyganek and Siebert [11] finding the global minimum is *NP-hard*. The related work in Chapter 3 gives an introduction into solving those optimization problems.

Disparity refinement

Disparity refinement can be seen as an optional post-processing step some algorithms perform automatically or may be requested manually. Refinement steps can also be implemented independently from the algorithm as they are executed on the final disparity maps. Sometimes the literature mentions those as clean-up steps. Here is a list of some known refinement steps:

- Sub-pixel estimation for higher accuracy.
- Disparity verification with left-to-right and right-to-left disparity map comparison (can also detect occluded areas).
- Filtering of disparity values, for instance using a median filter to remove mismatches.
- Interpolation of missing values: can be necessary when using an algorithm which produces a sparse disparity map.

Simplified block matching

For demonstration purpose of a working local disparity algorithm, block matching, also known as area matching, is sketched in a simplified version. The following algorithm assumes rectified images. Thus, the algorithm is executed along the scanlines.

1. Divide the images in blocks of the size $m \times n$ (e.g. 8×8).
2. Find the corresponding block along the scanlines as shown in Figure 2.10, i.e. the block with the lowest matching cost (e.g. sum of absolute differences).
3. Calculate for this block the displacement (the shift from left to right image) which results in the disparity.
4. This yields in the final, ideally *bijective*[14] disparity map after finding the corresponding block from the left to the right image and vice versa. If a block could not be matched the bijective criteria is not fulfilled.

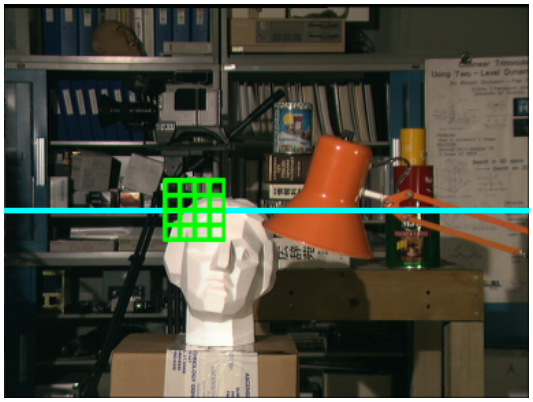

Figure 2.10: Illustration of block matching along a scanline.

In general, block matching leads to more accurate results with smaller window sizes. A bigger window leads to more smoothing which results in lower noise. The window size depends on the image size and its content. Therefore, no general assumption can be made. For each scenery the window size should be adjusted individually.

[14] Considering two sets, for each element of the first set a corresponding element of the second set is found. It also holds that both sets contain the same amount of elements. Thus, it is a one-to-one correspondence which also works inversely.

2.5 Sub-pixel accuracy

As seen in the sections before the disparity algorithms produce a disparity map consisting of integer values only. For most of the imaginable applications integer values should be enough. However, the world is continuous and there are applications which rely on accurate disparity estimations. For instance, having no sub-pixel values, image-based rendering produces an image for visualizing the disparity map, which can appear to be made up of many thin shearing layers [40]. To get an accurate sub-pixel value, the most common technique is to use curve fitting by utilizing an *n-th* polynomial-order function. In this particular case [40], a second-order polynomial function, i.e. a parabola is used. The curve is fitted around three or more values of the matching measure. The point of interest lies in the center of the chosen window (as Figure 2.11 depicts). The minimum of this parabola is the searched value [11, 41].

Curve fitting with a second-order-polynomial in figure 2.11 works with three data points: (d_{i-1}, m_{i-1}), (d_i, m_i) and (d_{i+1}, m_{i+1}). d_i is the found integer value for disparity and m_i is a match value for the displacement d_i. With the curve fit a new minimum value d_x is found which no longer needs to lie on the integer grid.

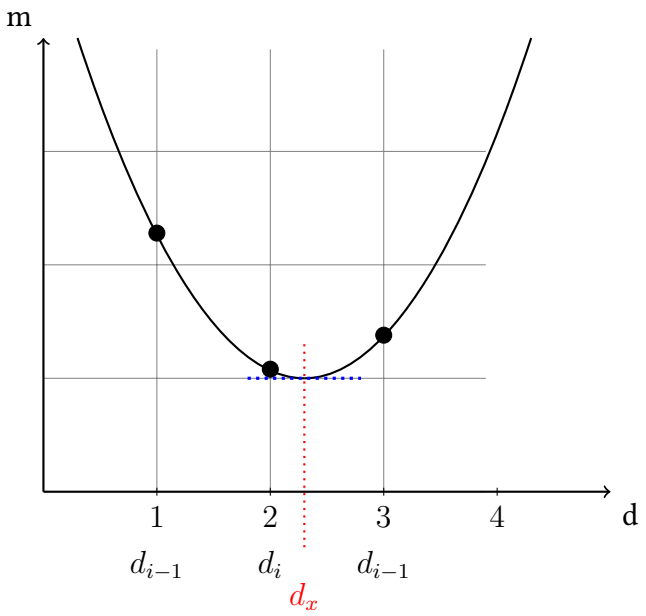

Figure 2.11: Sub pixel estimation of a disparity value around adjacent pixels.

2.6 Optical flow

Similar to the problems discussed in the section before, optical flow is also an image matching problem. The optical flow is defined as vectors describing small local displacements like moving objects or camera motion between two consecutive frames [7, 11]. The principle of the matching problem of images is comparable to disparity algorithms. The main difference is that instead of analyzing left and right image, a scene is investigated and the disparity describes small local vectors. To be more precise, the optical flow relies on the assumption that a certain point (x_1, y_1) in a frame at time t_1 will be matched to a point (x_2, y_2) in a frame at time t_2. Different approaches for estimating the optical flow of pixels exist, like:

- Correlation or block-matching,
- feature tracking,
- energy-based methods, or
- gradient-based methods.

Optical flow is heavily used in autonomous driving, automated traffic surveillance systems and video compression like H.264 [10, 31, 35, 38]. Recently a dataset containing ground-truth data of real-world sceneries regarding optical-flow information was released by Kondermann et al.. Figure 2.12 shows an example of estimating the movement of a vehicle. In the left image of Figure 2.12 most of the vectors are null as no local displacement can be estimated. Only a few vectors (small white dots) near the vehicle illustrate the displacements.

Figure 2.12: Optical flow estimation to obtain motion vectors (left) and pixel velocity magnitudes (right).[15]

[15] Source (accessed 02/2016): `http://de.mathworks.com/discovery/optical-flow.html`.

3 Related work

In this chapter the related work regarding disparity algorithms is treated. As integration of some disparity algorithms for the later evaluation was part of this thesis, the ones which were actually implemented are examined in more detail. The well-known semi-global matcher by Hirschmüller is introduced and the OpenCV implementations are mentioned. An approach by Geiger et al. to enable fast matching of high-resolution images is discussed. Both approaches utilize local methods for estimating disparity maps. One candidate adopting global methods is the Middlebury MRF library, which is also introduced in this chapter. This implies solving optimization problems (i.e. the minimization of a global energy cost function). Thus, the methods implemented by the library to solve such optimization problems are outlined. In the end, a short outlook on spatiotemporal consistency regarding disparity algorithms applied on videos is presented.

3.1 Semi-global matching

Hirschmüller combines two different methods, global- and local-matching for determining accurate disparity at a lower runtime as other global algorithms, which tend to run pretty long on current hardware [20, 21].

The semi-global matching (SGM) method utilizes pixel-wise matching of so called mutual information (MI) via entropy H, their joint-entropy of a pair of images and combining those with the approximation of a global two-dimensional smoothness constraint:

$$MI_{I_1,I_2} = H_{I_1} + H_{I_2} + H_{I_1,I_2}. \tag{3.1}$$

The previous discussed one-dimensional constraints are applied as well. Calculating the matching cost based on mutual information is insensitive to recording differences and illumination changes [20, 46]. The joint entropy H_{I_1,I_2} is low (meaning low information content) for rectified images as one image can be predicted by the other. The MI matching cost are defined as the following:

$$mi_{I_1,I_2}(i,k) = h_{I_1}(i) + h_{I_2}(k) - h_{I_1,I_2}(i,k), \tag{3.2}$$

where h_1 and h_2 are calculated from the probability distribution of corresponding intensities. Thus, $h_{I_1,I_2}(i,k)$ serves as the matching cost for the two intensities i and k. The idea then is, that one image needs to be warped[1] such that corresponding pixels are at the same location in both stereo images:

$$I_1 = I_b \quad \text{and} \quad I_2 = f_D(I_m), \tag{3.3}$$

where I_b is the base image, I_m the match image and $f_D(x)$ is a function which outputs the matching corresponding point. As the matching cost represent the information content of two intensities I_1 and I_2, which should be low (i.e. as equal as possible), the disparity map D needs to be known *a priori* for warping. Hence, the MI matching cost needs to be calculated either iteratively or hierarchically. On the one hand, an iteratively approach utilizes a random disparity image for calculating the MI matching cost, which serves as the base for the next iterations. On the other hand, the MI matching cost can be calculated hierarchically by recursively using an up-scaled disparity image, which has been calculated at half resolution with a common similarity measurement like SAD. For a deeper explanation of how the mutual information are exactly calculated and used in the SGM method compare [20–23].

OpenCV BM and SGBM

The OpenCV library [7] offers with its current version 3.1.0 two implementations for disparity estimation, block matching and semi-global block matching based on the idea of Hirschmüller. This version also contains a new filter, which was initially introduced with version 3.0.0, named *Disparity WLS Filter*[2]. WLS stands for weighted least squares (in the form of a fast global smoother). This disparity filter smoothes the disparity and also performs a left-right-consistency check to refine the results in especially half-occluded and uniform areas [36]. This yields to better and more accurate results but has the drawback of loosing negative disparity values. Negative disparity can appear if the stereo cameras are verged or inclined towards each other. The WLS filtering results in disparity ranging from 0 to D_{max}, as set before. Thus the negative disparity is -1.

[1] In this context warping can be seen as a function which maps pixels from the destination image to pixels in the original image. Then the pixels are copied at the mapped position to the coordinates in the destination image.

[2] `http://docs.opencv.org/3.1.0/d9/d51/classcv_1_1ximgproc_1_1DisparityWLSFilter.html`

3.2 ELAS: Efficient large-scale stereo matching

Geiger et al. proposed a novel approach for estimating the disparity with so called support points [15, 16]. A support point is like a feature, a point which can be robustly matched. For those support points a sparse disparity map is calculated. For more robustness, only the support points which can be matched left-to-right and right-to-left are retained. To remove ambiguities, the ratio between the best and the second best match of all points is taken into account. If the ratio exceeds a fixed threshold, the points are removed. Support points which have a different disparity value than all adjacent points are outliers and removed as well. As the found support points may not cover the whole image, additional support points in the image corners are added. They adopt the disparity value of their nearest neighbor. Then, image coordinates of the remaining support points are used to create a 2D mesh via Delaunay triangulation. To obtain a dense disparity map missing disparities are interpolated using mesh of the Delaunay triangulation by using the nearest-neighbor on the same image line. For more information how the support points get calculated and how the interpolation is done exactly, compare [15, 16].

3.3 Middlebury MRF library

The Middlebury MRF library [41, 43] utilizes a global energy function consisting of Markov random fields to formulate an energy minimization problem and offers the following methods to solve this optimization problem:

1. iterated conditional modes (ICM),
2. graph cuts expansion approach (cf. [5, 6, 30]),
3. graph cuts swap approach (cf. [5, 6, 30]),
4. sequential tree-reweighted max-product message passing (TRWS) (cf. [29, 47]),
5. sequential belief propagation (BPS) (cf. [6]),
6. max-product belief propagation (BPM) (cf. [6]).

The following subsections give a rough overview on some of those methods. Additionally, a short introduction into MRF-based energy functions is given. Also, the generalized concepts of how the above techniques help to solve such optimization problems are outlined.

3.3.1 Solving optimization problems

Many problems in computer vision can be described in terms of energy minimization for instance image smoothing, the stereo correspondence problems as described in Chapter 2 and many other. Thus, solving of optimization problems is a key part in modern stereo matcher algorithms. They solve the labelling problem as described in Chapter 2. Most of the current disparity algorithms are using global methods to solve an energy minimization problem. Usually they utilize Markov random fields (MRF) based energy functions. As such MRF based energy functions are *NP-hard* approximation algorithms like the following are typically used [11, 45]:

- dynamic programming,
- belief propagation,
- graph cuts.

All of these methods have in common that they are supposed to solve so called inference problems, or at least approximate those. Markov random fields, mentioned before, is also called Markov network. Bayesian networks as well as Markov networks are so called graphical models. Such graphical models help to understand the reasoning behind those formulations and to actually build algorithms which solve those inference problems. Both networks express the dependencies of nodes as the conditional probability. A chain of nodes is the so called joint probability. This is then the product over-all (joint) probabilities. The goal of algorithms which solve inference problem is to compute certain marginal probabilities, i.e. the probability that some pixel reaches a specific label node [11]. With inference the computation of these marginal probabilities is meant. Marginal probabilities are defined as the sums over all possible state of all the other nodes in the system. They are also called beliefs [50].

Markov random fields

Markov random fields (MRF), also called Markov network, are used to formulate problems in a probabilistic way represented as an undirected graph consisting of random variables, see 3.2. A MRF is a graph $G = (V, E)$ with $V = 1, 2, ...N$ denotes a set of vertices or nodes. Each node is associated with a random variable u_j for $j = 1...N$. E describes the edges $(i, j) \in E$ between the nodes i and j. The neighborhood of a node i is the set of nodes to which the node i is adjacent, i.e. $j \in N$ if and only if $(i, j) \in E$. The neighborhood of a node i is denoted as N_i. The Markov random field satisfies:

$$P(u_i \mid \{u_j\}_{j \in VN}) = P(u_i \mid \{u_j\}_{j \in N_i}), \tag{3.4}$$

where N_i is the so called Markov blanket of node i. It describes that the graph should be conditionally independent of all of the other variables given its neighbors. A hop from one node to another can be seen as a chain of probabilities which have to occur, also called Markov chain. The main idea behind MRF in combination with computer vision problems is to formulate the so called labelling problem in such a way, that each pixel has a likelihood to belong to a certain label [44]. The core problem then is to find exactly one label for each pixel, represented as a node in a MRF. This label represents then the optimal solution to an underlying problem, in the case of stereo correspondence, the disparity for a pixel [11].

In contrast to MRF there also exist Bayesian networks. A Bayesian network is a directed graph there as MRF is undirected. This implies two important aspects, the direction of a certain probability to hop from one node to another. MRF can not represent induced and non-transitive dependencies. Two independent random variables may be connected by an edge because of possible dependencies. Bayesian networks overcome this limitations.

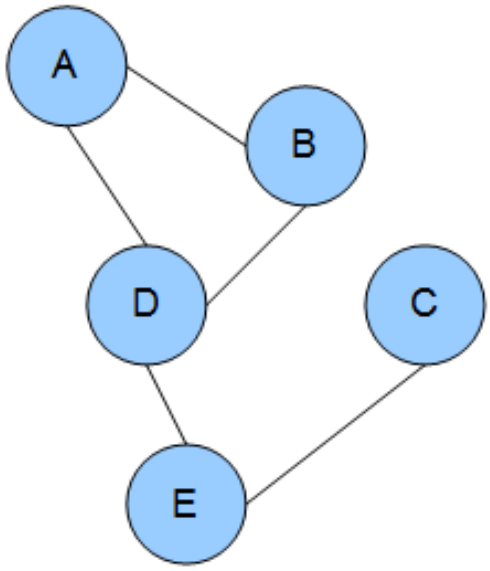

Figure 3.1: Example of Markov random fields[3]

[3]Source (accessed 03/2016): `https://en.wikipedia.org`.

Factor graph

As those problems are *NP-hard*, there exist several approximation algorithms which are outlined in the following subsections. All of these approximation algorithms work on so called factor graphs. A factor graph represents a factorized function and is bipartite[4]. A MRF function is factorized in partial functions and then formulated in a factor graph. The solution to the problem represented by the factor graph is then approximated. An important notion of factor graphs is the message which can be passed from a node to another. There a few exceptions, if the factor graph contains no cycles, the solution can be exact computed with message passing (also called belief propagation) algorithms which work on a tree. Otherwise only an approximation is possible.

Dynamic programming

In general, dynamic programming means having an optimization problem which can be parted into smaller chunks. Then these chunks get solved individually and in the end, these chunks are connected and the optimization problem is minimized [1, 2, 11]. For stereo matching this applies to the partition of a two-dimensional search problem into a series of isolated one-dimensional search problems on each pair of epipolar lines. These problems are then solved independently. With dynamic programming the following energy function (introduced in the foundations Chapter 2 can be solved independently per scanline.

$$E(d) = E_{data}(d) + \lambda E_{smooth}(d) \tag{3.5}$$

Dynamic programming has two benefits, it is solvable efficiently in polynomial time and it enforces the ordering constraint (as it is solved per scanline). But it can lead to streaking effects, meaning that the result image seems to be constructed of many independent layers.

Belief propagation

Belief propagation is in general a technique to perform inference on a probabilistic model like Bayesian networks or Markov random fields [11, 45, 50].

Graph cuts

For approximating problems formulated in a Markov random field there also exist so called graph cuts algorithms [6, 11]. In general, graph cuts work like the

[4] If the nodes of a graph can be divided into two disjoint sets, for instance U and V, such that every edge connects a node U to one in V, then the graph is bipartite.

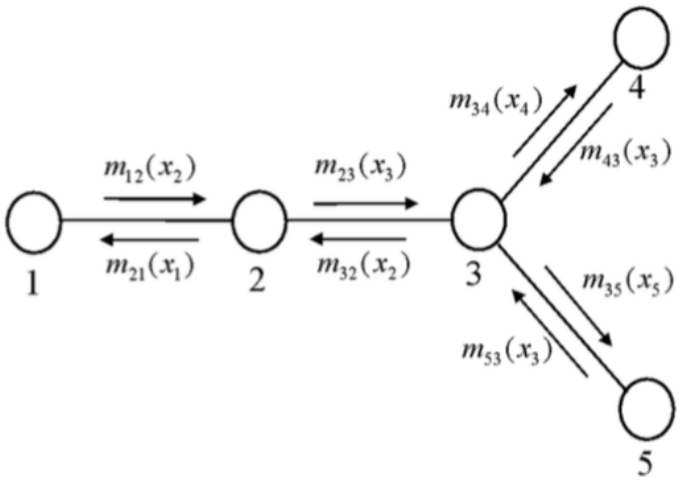

Figure 3.2: Illustration of messages passed in BP [50].

following: assuming a graph G with nodes N and some edges E. The goal is to delete enough edges so that each pixel is connected to exactly one label node. Given a weighted graph G with source s and sink t nodes. The graph should be partitioned into two sets, S and T, where $s \in S$ and $t \in T$. This set presents a subgraph such that the sum of edge weights spanning this partition is minimized.

In the case of computer vision graph cuts is used as the following:

There exist two algorithms to solve such a graph:

- α-expansion algorithm, and
- α-β-swap algorithm.

3.4 Spatiotemporal consistency

Although stereo correspondence is a research field which has been heavily investigated for a few decades no real disparity algorithm for videos exists yet. One reason for that can be the lack of solid ground-truth data. Only a few datasets has been introduced lately [8, 41]. However, a novel approach was presented by [39], [28] and [24]. The basic idea behind all of those presented approaches is to handle occurring noise.

Explain how the video restoration algorithms work (basically). They added noise. Blablabla.

- Small description what is currently available.
- What can we do?
- Explain why some stuff is not available at all.
- Also point out the lack of ground truth data. This is a huge problem.
- Link to datasets!

4 Implementation

Chapter 3 pointed out that no real algorithm for stereoscopic video disparity exist yet. Other issues for more research in that area are:

- No evaluation engine for videos exist yet.
- Currently only little datasets regarding ground-truth data for stereoscopic videos are available.

Thus, the decision towards an own evaluation engine was made. In this chapter the implementation, its components and the novel approach concerning the subsequent optimization of disparity maps are described.

4.1 Preliminaries

As development platform a MacBookPro was used with the following specifications: i5-4258U CPU @ 2.40GHz, 8 GB RAM, a fast SSD. Everything except the web result viewer was implemented using C++. As a timer saver and for reducing code duplicates OpenCV as master library was used. Everything is based on OpenCV. In addition the Boost library was used for some simple tasks like creating an array of arbitrary length for keeping a simple binary state or parsing the command line options. The build-chain consists of some shell scripts and CMake as makefile generator. With CMake it was possible to cross-compile the app for Linux and use a fast server-instance from DigitalOcean[1] for the generation of the disparity maps and to actually evaluate those.

4.2 Overview

Initially, a rapid monolithic prototype was built featuring the execution of different disparity algorithms, the creation of bitmasks and the evaluation of a given scene with different parameters. But as more datasets were found and various bitmasks as an evaluation method were established the need for a leaner process chain arose. Especially as disparity algorithms need some time to compute the disparity map

[1] `https://www.digitalocean.com`

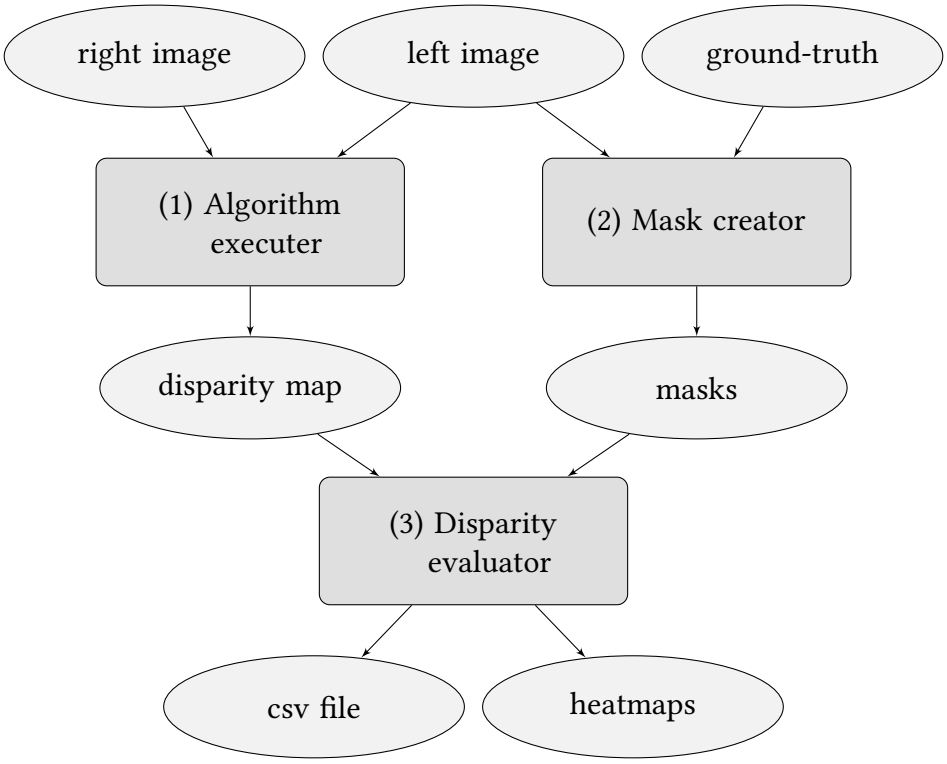

Figure 4.1: Processing pipeline of the implementation.

for one frame. Hence, as videos consist of multiple frames (in our datasets about 90 frames in mean) this is a time consuming task. Sometimes metrics change or a new metric is established, the threshold can be adjusted. These are the reasons for an approach towards microservices with which computed disparity maps can be evaluated repeatedly and independently. Thus, the monolith was rewritten partitioned in smaller microservices shaping four different components:

- DisparityAlgorithm,
- PostDisparityMapSmoothing,
- BitmaskCreator,
- DisparityMapEvaluationSuite.

The figure 4.2 shows the composition and figure XXX the evaluation chain of these microservices. The output which each one of those microservices in the chain can generate or operate on is structured in a simple folder tree:

- /datasets/{dataset_identifier}/{dataset_sequence_identifier}/{appendix}

There {appendix} can be either {disparity_maps_computed}, {disparity_maps_-smoothed} or {bitmasks}.

The computed disparity maps are saved in a binary format since OpenCV is currently not able to use the OpenEXR file format properly (only reading is possible). Hence for visualization they have to be normalized in the range of 0-255 or may be presented as a heat map. The evaluation is done with simple python scripts reflecting the evaluation chain.

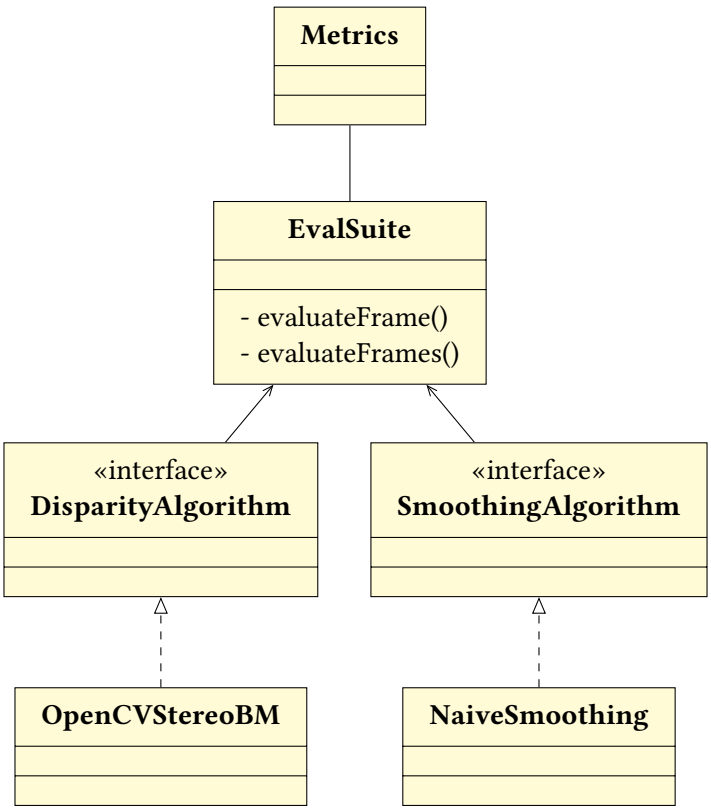

Figure 4.2: Simplified UML diagram of general architecture.

4.3 Disparity algorithms on images

Deciding which algorithms should be describe was not an easy task. On the one hand, the algorithms which shall be implemented during this thesis are important and thus should be described definitely. On the other hand, there is a huge diversity of used technologies amongst disparity algorithms. For instance various programming languages, the decision between cpu- versus gpu-rendering, differ-

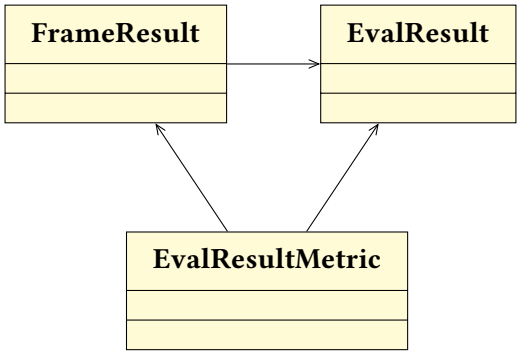

Figure 4.3: Simplified UML diagram of result composition for further processing.

ent coding styles and used libraries. As a matter of fact, this makes it harder to implement and then evaluate every single disparity algorithm. Thus, the algorithms from Middlebury were integrated in the evaluation suite and streamlined. Additionally, the so called efficient large-scale stereo matcher (ELAS) was also integrated. The parameters used for each algorithm are described in the implementation chapter. This section is for giving an overview on these algorithms as well as their parameters for the later implementation chapter 4.

4.4 Disparity algorithms on videos

At the current point in time, no real disparity algorithm for especially videos exists yet. As a video is defined by multiple consecutive frames, every disparity algorithm for images can be applied on videos. The drawback of this trivial approach is the lack of taking the correlation of the frames into account. None the less it is possible to focus on some other details, for instance:

- possible outliers in the sense of frames,
- mean performance (error rate) of those algorithms on a complete scene,
- runtime variety in a sequence,
- analyzing the impact of noise, and
- trying to smooth noisy areas in the resulting disparity map with other frames.

Noise can occur through video compression. As video sensors tend to be noisier than image sensors it also more present in stereoscopic videos, if not rendered by a computer. As noise can be simulated and added onto the rendered video, it is

investigated how noise disturb stereo matcher. As these ideas are more explained in the implementation chapter 4 the following subsection a novel approach for videos are examined.

4.5 Evaluation engine for videos

In contrast to other implementations, input and output are clearly defined and thus different techniques can be adapted easily. There exist combined frameworks which fulfill two tasks, disparity calculation (as the algorithm is implemented) and the final evaluation step. This makes it harder to use the evaluation module separately from the rest. None the less the open source community around computer vision also lacks of code for stereo matcher. Due the diversities of algorithms and eval suites the decision was made to go for an OpenCV implementation of an eval suite for disparity algorithms.

Works basically as a wrapper. Can output statistical stuff. Basically works on disparity maps / images.

Huge mistake could be to apply the metrics on the whole disparity map from the algorithm. The output contains areas which are black (value = 0). This can be:

- noise
- mistaken be the algorithm
- expected disparity
- non-occluded areas

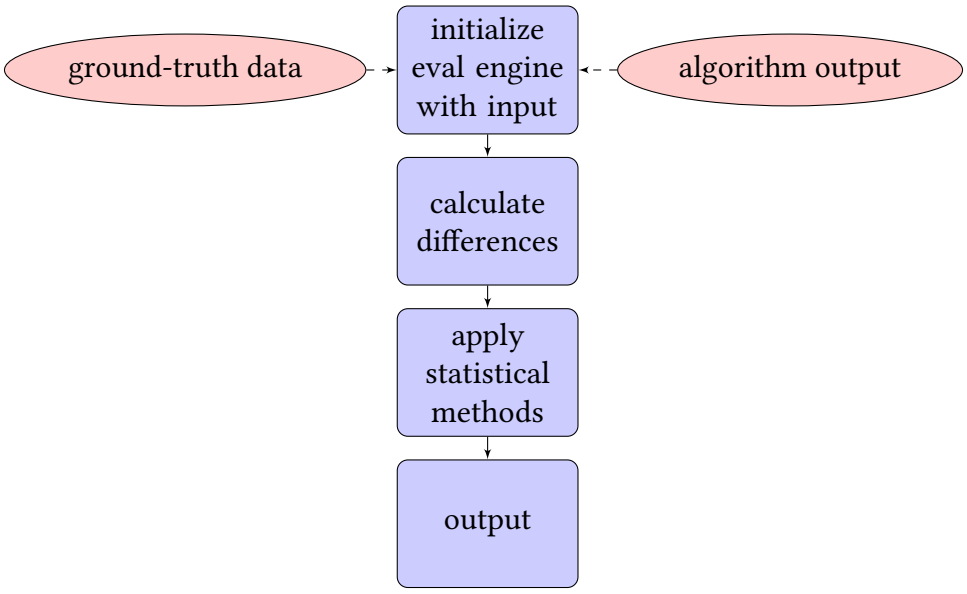

The eval engine has two modes to be queried:

- via command-line which also results in a console output,
- with a configuration file ($config.json$) which leads to an output in a given folder for the web result viewer.

4.6 Preprocessing

Different tasks are executed before the actual disparity algorithm are invoked and the evaluation takes place:

- Normalization
- Gaussian noise

Normalization

No clue.

Gaussian noise

randn[2]

[7]

As seen in the related work chapter 3, some approaches use restoration algorithms in order to reduce noise which can occur. Hence noise generation was added as a preprocessing step in order to see how noise disrupts disparity algorithms. We use gaussian noise meaning that the noise is gaussian-distributed.

$$f(x) = ae^{-\frac{(x-b)^2}{2c^2}}$$

$$p_G(z) = \frac{1}{\sigma\sqrt{2\pi}} e^{-\frac{(z-\mu)^2}{2\sigma^2}}$$

In this example, z represents the grey level which is added to the image matrix later on. μ is the mean value (= 0). σ is the standard deviation.

The σ can be set in our evaluation suite in order to see how this distracts the image.

[2] `http://docs.opencv.org/master/d2/de8/group__core__array.html#gaeff1f61e972d133a04ce3a5f81cf6808`

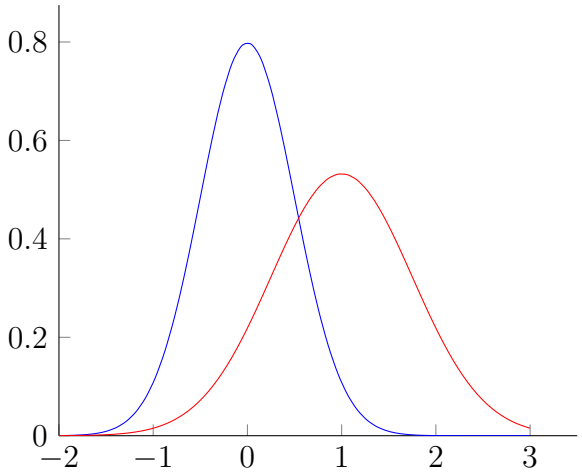

4.7 Fine-grained evaluation via bitmasks

The evaluation would be trivial by just comparing the computed disparity map with its ground-truth companion. This trivial comparison would be a pitfall, as the results would be erroneous due to for instance unknown disparity or occluded regions. As remedy bitmasks are introduced to simply focus on interesting pixels. In this section the following bitmasks are introduced and how they are calculated:

- Depth-discontinuity
- Textured regions recognition
- Discover occluded pixels
- Saliency detection
- Unknown disparity

First describe the motivational introduction to bitmasks why would one use those?

Depth-discontinuity

Determining correspondence can fail in textureless or depth-discontinuous regions as mentioned above. Thus it is also interesting how the algorithms handle such regions. For this purpose a depth-discontinuity mask was implemented as well.

Explain:

- Dilate

- Erode
- maybe show short example image (combined dilate/erode)
- explain how the bitmask is calculated

Textured regions recognition

As stereo matching algorithms act on the assumption that the disparity is smooth, especially if contrast and color intensity do not change drastically, it can be interesting to see how those algorithms treat textured and textureless regions. Thus a bitmask for textured regions recognition was implemented.

Explain (shortly):

- Sobel
- pow
- boxFilter
- how we get the bitmask

Discover occluded pixels

An occluded pixel is defined as a pixel which is hidden in one of the two images, for instance an object hides it from a different angle. In the case of stereo matching the disparity can not be calculated for such a pixel. Thus occluded pixels have to be handled properly, as they could distort our result. For this purpose a simple mask is introduced to indicate which pixels on the scene are visible for both cameras and which are not.

Explain and cite two papers (taxonomy of disparity algorithms). There it is explained how everything is working. Explain how the get the result (use algorithm).

Thus we need to take care about non-occluded areas. For this purpose we generated bitmasks (the size w * h) for each video dataset.

"In addition to disparity maps, for stereo matching method evaluation it is interesting to have a non-occluded area mask. This mask represents in white color the pixels on the scene that are visible from both cameras and in black color the pixels that are visible from only one camera. To obtain the non-occluded area mask, we simply cross-checked the left and right disparity maps. Pixels that are visible in both cameras will have the same value in both disparity maps, but for occluded pixels the left and right disparity value will be different. The performance of the stereo matching algorithm on areas where pixels are occluded is one of the

most important quality indicators of the algorithm, as it is very difficult to find the matching point of a pixel in one of the images if it is not visible on the other image." [34].

Saliency detection

Another criteria for the later evaluation is how the algorithms operate on regions which are salient in a specific scene. There exist some algorithms for saliency detection in either images or videos [7, 13]. OpenCV offers two different saliency categories to be computed:

- $StaticSaliency$ in images, and
- $MotionSaliency$ on videos.

Explain how saliency detection works, implemented via OpenCV. Otsu's algorithms, threshold and K-Means algorithm [25].

Unknown disparity

Is -1.

4.8 Integration of existing algorithms

Figure 4.4: Basic integration of existing algorithms

This does not exist currently, so we use the Middlebury Test Suite with its algorithms for images and apply them on videos.

- Consists of multiple steps
- Wrapper to call different algorithms
- normalizing of output
- actual eval process

Input: ImageLEFT, ExpectedLEFT, ImageRIGHT, ExpectedRIGHT Output: a good metric for showing good/bad disparity, a few ideas.

4.9 Postprocessing

Postprocessing only consists of one task: normalization of the disparity map. Some algorithms struggle with calculating a larger number than the number of disparities of 32. Some datasets only calculated the disparity to be in a range from 0 to 63. Grayscale normally ranges from 0 to 255. Thus the disparity map is normalized to range from 0 to 63.

Simply only disparity normalization.

4.10 Web result viewer for evaluation suite

For fine-tuning the algorithm's parameters as well as implementing the bitmasks it was helpful to see the visual output of both. As the resulting bitmasks for each frame with the computed result disparity map were saved on the hard-drive for further investigations a web result viewer was created for visualizing the output. The following features were implemented:

- Starting new computations with different parameters and scene selection.
- Playing frame-by-frame with different speeds.
- Online csv-export of result.

- Insert screenshot (one or two from web result viewer)
- Describe basic features
- Describe what could be done with the evaluation web suite in near future
- But for thesis evaluation a csv exporter was used.

4.11 Processing huge amount of data

- Swarm
- Bees
- spawn workers with docker
- aggregate results

Especially a docker image was created[3].

[3] `https://github.com/benjohnde/dockerbase-opencv`

« Result-Viewer

Comparison of Disparity Algorithms for Stereoscopic Video

QUEUE NEW

Timestamp	sessionId	Algorithm	ImageSet	Smoothing
2016-01-24T19:11:26.000Z	f792db42-34d9-45c7-8202-73631c4d55a5	3	book/	
2016-01-18T12:13:06.000Z	32dacd05-1680-4b96-ac8c-341e5411daec	4	street/	
2016-01-18T11:55:19.000Z	08e6aafa-5c50-4981-9ad2-5b761bcdedf4	1	book/	
2016-01-18T11:50:47.000Z	4d9b69d9-a5f4-4a51-93cd-31ef08838c8c	1	book/	
2016-01-18T11:47:10.000Z	4968e819-ed4e-4f09-b373-9b869992f336	3	book/	
2016-01-18T11:43:32.000Z	24ed2505-7799-469e-a54c-10256efdfe67	1	book/	
2016-01-14T22:16:50.000Z	115c51eb-5192-47b9-b815-38c0debb62ad	3	book/	

Figure 4.5: Overview page of web result viewer.

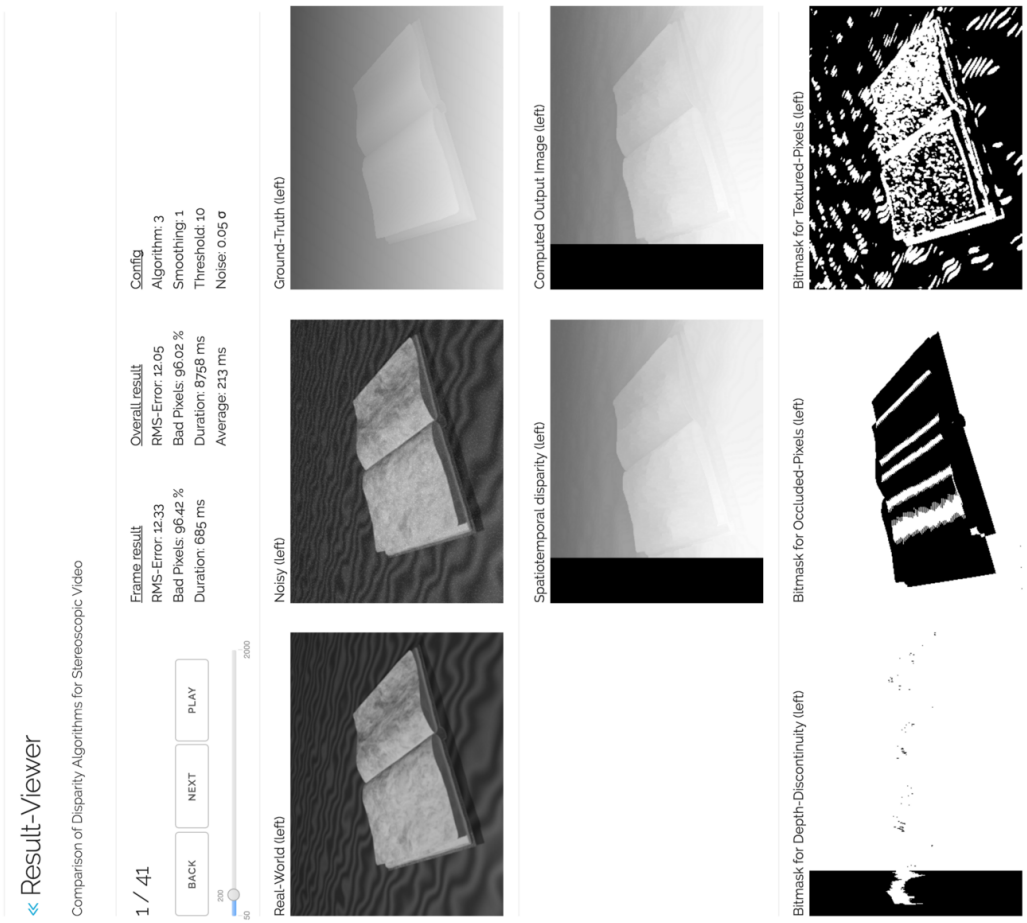

Figure 4.6: Detail of one result in the web result viewer.

4.12 Discussion

The following modules were actually implemented:

- Reader for the PFM file format.
- Python scripts for upcoming evaluation.
- Shell scripts for getting the docker containers and thus the work distributed among different instances[4].
- Evaluation processor for

[4]With instances virtual machines from DigitalOcean are meant.

5 Evaluation and results

Short outline as usual.

5.1 Datasets

- Tsukuba Stereo Dataset (used Tsukuba Map as reference)
- Stereo videos with ground truth disparities from cambridge[1]
- SVDDD - a high-resolution Stereoscopic Video Dataset with precise Depth and Disparity information

Ground-truth data

In general there exist two ways to gain ground-truth information of pixels:

- in the real-world sense the area,
- in computer-animated scenes let the renderer calculate the disparity.

The former can be achieved via area scanner for instance a radar. This approach is of course more error-prone than the latter one. It can lack of accuracy due to false measurements. The latter one provides real ground-truth information.

Provide real-world ground truth disparity maps [31].

Availability

The aim of such datasets is to provide data which we can rely on to evaluate the performance of computer vision algorithms, such as disparity algorithms in this thesis. Without having such datasets it would be crucial to rate the overall quality of for instance stereo matching algorithms.

We use the datasets for stereo correspondences from Middlebury, cf. [41]. They provide us with three examples. Each of those examples include an image from each camera (left, right) and the resulting ground-truth disparity map.

[1] `http://www.cl.cam.ac.uk/research/rainbow/projects/dcbgrid/datasets/`

We also use the small images from [34].
Famous Tsukuba ground-truth dataset:

- 64 levels of disparity, so grayscale image
- generated scenes with Autodesk Maya 2012

[34]
Ground truth data? How to provide such data?

Tsukuba stereo dataset

This dataset can be seen as the origin of stereoscopic datasets. The first dataset ever released for working with stereoscopic images. [34].

Middlebury stereo dataset

[41].

Cambridge stereo dataset

The Cambridge stereo dataset consists of five different rendered scenes in $400x300$ resolution with each about 100 frames [39]. The dataset scales the disparity for each scene from 0 to 64.

SVDDD - a high-resolution Stereoscopic Video Dataset with precise Depth and Disparity information

The Lehrstuhl für Praktische Informatik IV[2] has created a novel dataset on its own containing depth information for stereoscopic videos. Before the evaluation it was clear that this dataset is going to be evaluated as well. The difference is that this dataset was not analyzed before. Thus it is possible that the chosen algorithms work not properly on this dataset. If this case occurs there exist two possibilities why this happens:

- On the one hand, the disparity information are not properly calculated, or
- on the other hand, those algorithms have some troubles with the constructed scene.

[2] `http://ls.fmi.uni-mannheim.de/de/pi4/`

Focusing on the latter one, the scenes were created with Blender and utilizes the XXX (insert me pls) open-source scenes. A second camera was added to the scene for obtaining depth information. The parameter for each scene can be extracted from the paper. The most important points which can lead to a discrepancy between the computed disparity maps and the ground-truth data are the following:

- rays of light were removed only in the ground-truth-data,
- motion and object blur was reduced only in the ground-truth data,
- fain-grained textures were reduced only in the ground-truth data.

5.2 Quality metrics

To evaluate the quality of computed disparity maps we need at first to what we compare the computed disparity maps to and secondly how to compare them. In the section **??** the availability of such datasets were discussed.

Insert table here.

Tag	Description
σ_{10}	Guassian noise calculator.

Table 5.1: Overview on used metrics in results

Typical quality measure instruments for comparing disparity maps against their ground-truth reference data are [11]:

- Percentage of bad matching pixels
- Root-mean-square error
- Parameter-free measures

In addition the following are also considered:

- Mean absolute error in pixels
- Error quantiles
- Precision and accuracy

Percentage of bad matching pixels

$$\text{PBMP} = \frac{1}{n} \sum_{x,y=0} (|d_a(x,y) - d_e(x,y)| > \delta_t) \tag{5.1}$$

Percentage of bad matching pixels for given threshold.

Root-mean-squared error

The mean squared error (MSE) as well as the root mean squared error (RMSE) are both the most popular metrics in image and video processing. The MSE is as the name implies the mean of the squared differences between the intensities of pixels in two pictures at the same position. In conclusion the average difference per pixel is then the root of the squared error.

$$\text{RMS-Error} = \sqrt{\frac{1}{n} \sum_{x,y=0} (d_a(x,y) - d_e(x,y))^2} \tag{5.2}$$

It represents the sample standard deviation of the differences between predicted values and observed values. Here $d_a(x,y)$ is the actual disparity value for given x and y. $d_e(x,y)$ is our expected disparity value from our ground-truth data. Hence the RMSE is the difference between values on average.

Energy efficiency

$$EE_{alg} = \frac{clean\ pixels}{runtime\ in\ seconds} \tag{5.3}$$

where $clean\ pixels$ are defined as bad pixels in percent of non-occluded pixels and $runtime\ in\ seconds$ the runtime for this particular frame. EE_{alg} is then calculated in the mean of all frames of a given sequence over all examined sequences and all datasets.

5.3 Measurement

- First took normal depth map images. But not that good, only values from 0-255.
- Actual evaluation process consists of comparison of real calculated values of depth map by results of algorithms.
- How does the eval actual look like?

[3], [40].

Parameter tuning

Our results.

Against reference dataset

It is also important to have some kind of reference dataset with which the evaluation engine can be calibrated with. Of course the settings (i.e. parameters of an algorithm) is dependent on the input material (size, noise) and on the scene (e.g. textured vs textureless). So it is possible to have good parameters for one scene and not for another. However, in order to evaluate those algorithms the Tsubuka stereo dataset was chosen as reference dataset to see how the eval engine actually works with the same parameters on the same images.

5.4 Results

The results are visualized with the HSV color model.

Figure 5.1: Scale of hue of the HSV color model.

Applying disparity algorithms on videos

As said in the implementation chapter 4 applying disparity algorithms on videos is trivial and straightforward. None the less different anomalies can be further investigated while analyzing videos:

- outliers in the form of a single frames which differs too much from the others,
- impact of noise,
- smooth the unknown disparity in frames (next subsection).

As you can see in the following result matrices the quality metrics regarding the salient regions are a bit esoteric. Of course there exist techniques to estimate

salient regions in static images and also in videos. In videos moving objects can be detected as salient, referring to motion saliency[7, 48]. None the less those bitmasks are a bit more esoteric in the sense of there is room for interpretation.

Rank	Method	Sequence	RMS-All	RMS-Noc	RMS-Sal	RMS-Tex	RMS-DD
1	StereoSGBM	SVDDD 02_rabbit	4.35%	5.43%	1.0 px	1.1 px	300ms
2	StereoBM	SVDDD 02_rabbit	4.35%	5.43%	1.0 px	1.1 px	300ms

Table 5.2: Result matrix of RMS for videos

Rank	Method	Sequence	Out-All	Out-Noc	Out-Sal	Out-Tex	Out-DD
1	StereoSGBM	SVDDD 02_rabbit	4.35%	5.43%	1.0 px	1.1 px	300ms
1	StereoSGBM	SVDDD 02_rabbit	4.35%	5.43%	1.0 px	1.1 px	300ms
1	StereoSGBM	SVDDD 02_rabbit	4.35%	5.43%	1.0 px	1.1 px	300ms
1	StereoSGBM	SVDDD 02_rabbit	4.35%	5.43%	1.0 px	1.1 px	300ms
1	StereoSGBM	SVDDD 02_rabbit	4.35%	5.43%	1.0 px	1.1 px	300ms
1	StereoSGBM	SVDDD 02_rabbit	4.35%	5.43%	1.0 px	1.1 px	300ms
1	StereoSGBM	SVDDD 02_rabbit	4.35%	5.43%	1.0 px	1.1 px	300ms
1	StereoSGBM	SVDDD 02_rabbit	4.35%	5.43%	1.0 px	1.1 px	300ms
1	StereoSGBM	SVDDD 02_rabbit	4.35%	5.43%	1.0 px	1.1 px	300ms
1	StereoSGBM	SVDDD 02_rabbit	4.35%	5.43%	1.0 px	1.1 px	300ms
1	StereoSGBM	SVDDD 02_rabbit	4.35%	5.43%	1.0 px	1.1 px	300ms
1	StereoSGBM	SVDDD 02_rabbit	4.35%	5.43%	1.0 px	1.1 px	300ms
1	StereoSGBM	SVDDD 02_rabbit	4.35%	5.43%	1.0 px	1.1 px	300ms
1	StereoSGBM	SVDDD 02_rabbit	4.35%	5.43%	1.0 px	1.1 px	300ms
1	StereoSGBM	SVDDD 02_rabbit	4.35%	5.43%	1.0 px	1.1 px	300ms
1	StereoSGBM	SVDDD 02_rabbit	4.35%	5.43%	1.0 px	1.1 px	300ms
1	StereoSGBM	SVDDD 02_rabbit	4.35%	5.43%	1.0 px	1.1 px	300ms
1	StereoSGBM	SVDDD 02_rabbit	4.35%	5.43%	1.0 px	1.1 px	300ms
1	StereoSGBM	SVDDD 02_rabbit	4.35%	5.43%	1.0 px	1.1 px	300ms
1	StereoSGBM	SVDDD 02_rabbit	4.35%	5.43%	1.0 px	1.1 px	300ms
1	StereoSGBM	SVDDD 02_rabbit	4.35%	5.43%	1.0 px	1.1 px	300ms
1	StereoSGBM	SVDDD 02_rabbit	4.35%	5.43%	1.0 px	1.1 px	300ms
2	StereoBM	SVDDD 02_rabbit	4.35%	5.43%	1.0 px	1.1 px	300ms

Table 5.3: Result matrix of outliers for videos

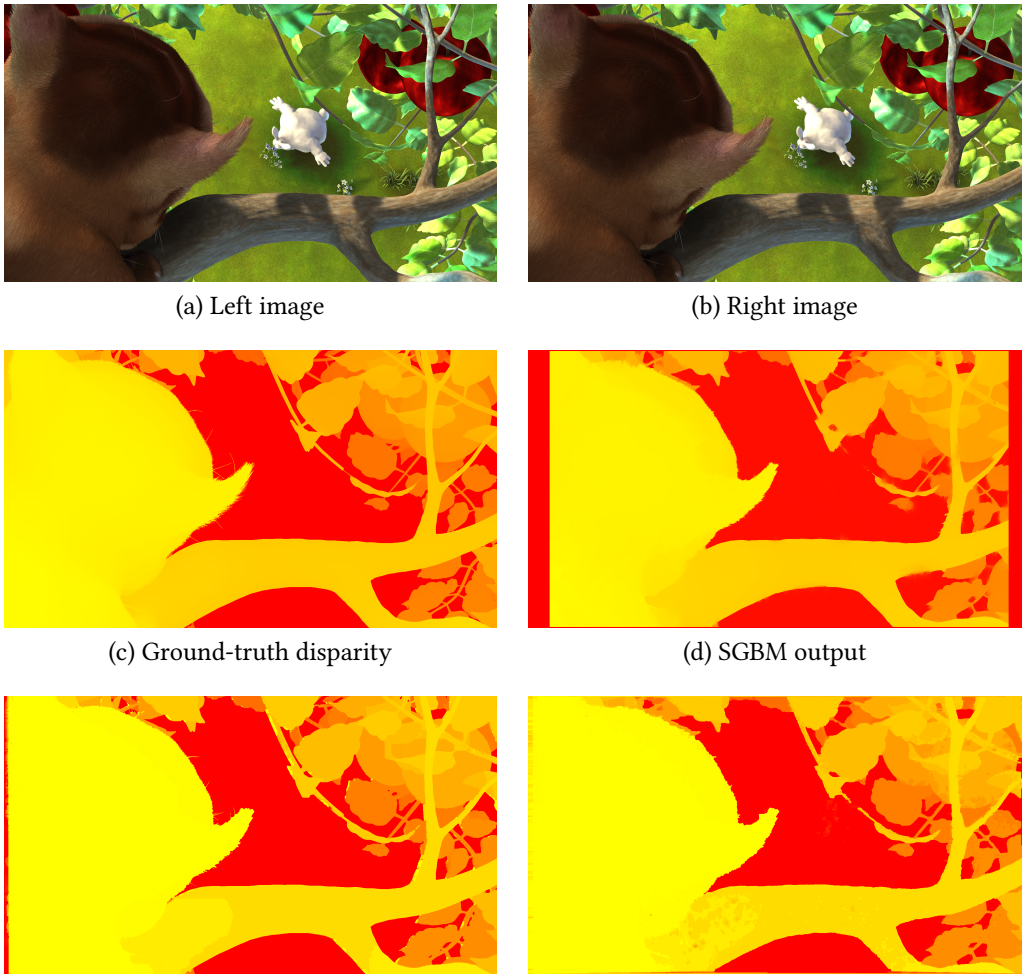

(a) Left image (b) Right image

(c) Ground-truth disparity (d) SGBM output

(e) MRF ICM output (f) ELAS output

Figure 5.2: Frame 01, scene 03 rabbit of the SVDDD dataset.

5.4.1 Smoothing over time

Result matrix

Insert overview matrix.

5.4.2 Runtime measurement

Depict:

- different performance of disparity algorithms,

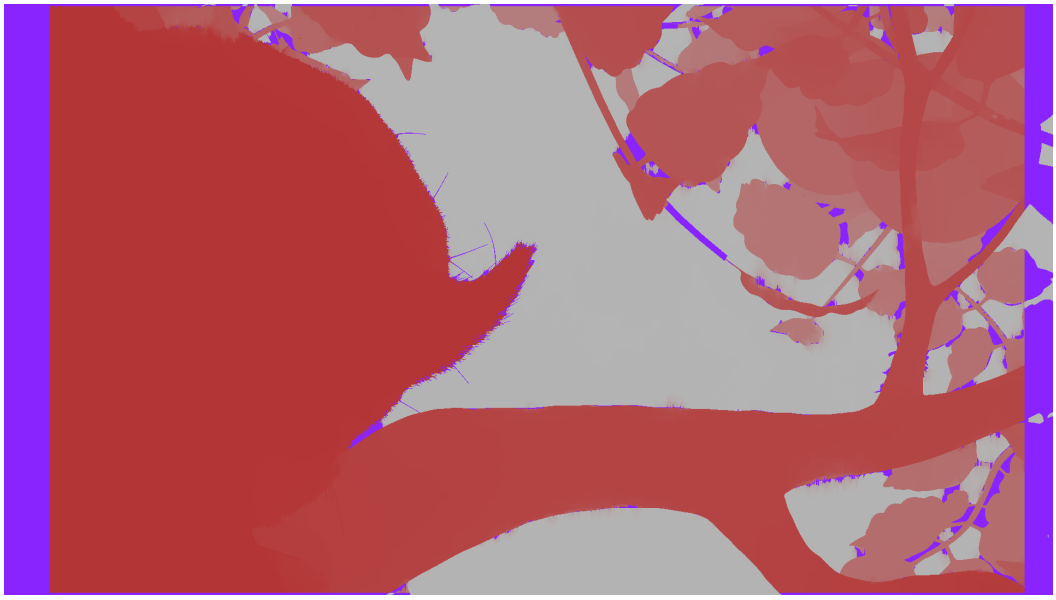

Figure 5.3: Heatmap of outliers with threshold of 4.0 pixels in computed disparity map with OpenCV SGBM, frame 01, scene 03 rabbit, SVDDD dataset.

- down-scaled performance,
- first down-scale, then run algorithms, then upscale, runtime,
- smoothing-over-time runtime.

Result matrix

Rank	Method	Sequence	Time	Time/MP	Quality index
1	StereoSGBM	SVDDD 02_rabbit	4.35%	5.43%	1.0 px
2	StereoBM	SVDDD 02_rabbit	4.35%	5.43%	1.1 px

Table 5.4: Result matrix of runtime for videos

5.5 Discussion

This is really important!

6 Conclusion

The work described in this thesis has been concerned with the comparison of disparity algorithms.

6.1 Thesis summary

- What the thesis brought with each chapter.
- One small paragraph regarding one disparity algorithm.
- One small paragraph regarding dataset of the chair.
- What was implemented.
- What the main result of the evaluation.

6.2 Future outlook

A few thoughts on possible future work to improve the presented algorithms, split in low- and high-level from a technical perspective:

Low-level

- Neuronal networks [37]
- Other matching cost calculation methods [19].
- Focus more on how humans experience depth? [12]

High-level

- Real-time availability
- higher resolution
- What's on the market, like multi-view?

- Provide more real-world ground truth disparity maps [16, 31].

Bibliography

[1] E. Angel and R. Bellman. *Dynamic programming and partial differential equations*. Academic Press, Inc., 1972.

[2] R. E. Bellman and S. E. Dreyfus. *Applied dynamic programming*. Princeton university press, 2015.

[3] A. Benoit, P. Le Callet, P. Campisi, and R. Cousseau. Quality assessment of stereoscopic images. *EURASIP journal on image and video processing*, 2008.

[4] B. Block and P. McNally. *3D Storytelling: How stereoscopic 3D works and how to use it*. Taylor & Francis, 2013.

[5] Y. Boykov and V. Kolmogorov. An experimental comparison of min-cut/max-flow algorithms for energy minimization in vision. *Pattern Analysis and Machine Intelligence, IEEE Transactions on*, 26(9):1124–1137, 2004.

[6] Y. Boykov, O. Veksler, and R. Zabih. Fast approximate energy minimization via graph cuts. *Pattern Analysis and Machine Intelligence, IEEE Transactions on*, 23(11):1222–1239, 2001.

[7] G. Bradski. The OpenCV library. *Dr. Dobb's Journal of Software Tools*, 2000.

[8] D. J. Butler, J. Wulff, G. B. Stanley, and M. J. Black. A naturalistic open source movie for optical flow evaluation. In A. Fitzgibbon et al. (Eds.), editor, *European Conf. on Computer Vision (ECCV)*, Part IV, LNCS 7577, pages 611–625. Springer-Verlag, Oct. 2012.

[9] M. M. H. Chowdhury and M. A.-A. Bhuiyan. A new approach for disparity map determination. *Daffodil International University Journal of Science and Technology*, 4(1):9–13, 2009.

[10] I. Cohen and G. Medioni. Detecting and tracking moving objects for video surveillance. In *Computer Vision and Pattern Recognition, 1999. IEEE Computer Society Conference on.*, volume 2. IEEE, 1999.

[11] B. Cyganek and J. P. Siebert. *An introduction to 3D computer vision techniques and algorithms*. John Wiley & Sons, 2011.

[12] G. C. DeAngelis, I. Ohzawa, and R. D. Freeman. Neuronal mechanisms underlying stereopsis: how do simple cells in the visual cortex encode binocular disparity? *Perception*, 24(1):3–31, 1995.

[13] T. Dittrich, S. Kopf, P. Schaber, B. Guthier, and W. Effelsberg. Saliency detection for stereoscopic video. In *Proceedings of the 4th ACM Multimedia Systems Conference*, pages 12–23. ACM, 2013.

[14] M. Fahle. Wozu zwei Augen? *Naturwissenschaften*, 74(8):383–385, 1987.

[15] A. Geiger, M. Roser, and R. Urtasun. Efficient large-scale stereo matching. In *Asian Conference on Computer Vision (ACCV)*, 2010.

[16] A. Geiger, J. Ziegler, and C. Stiller. Stereoscan: Dense 3D reconstruction in real-time. In *Intelligent Vehicles Symposium (IV)*, 2011.

[17] R. A. Hamzah, R. A. Rahim, and Z. M. Noh. Sum of absolute differences algorithm in stereo correspondence problem for stereo matching in computer vision application. In *Computer Science and Information Technology (ICCSIT), 2010 3rd IEEE International Conference on*, volume 1, pages 652–657. IEEE, 2010.

[18] D. B. Henson. *Visual fields*. Butterworth-Heinemann Medical, 2000.

[19] S. Hermann and T. Vaudrey. The gradient - A powerful and robust cost function for stereo matching. In *Image and Vision Computing New Zealand (IVCNZ), 2010 25th International Conference of*, pages 1–8. IEEE, 2010.

[20] H. Hirschmüller. Accurate and efficient stereo processing by semi-global matching and mutual information. In *Computer Vision and Pattern Recognition, 2005. CVPR 2005. IEEE Computer Society Conference on*, volume 2, pages 807–814. IEEE, 2005.

[21] H. Hirschmüller. Stereo processing by semiglobal matching and mutual information. *Pattern Analysis and Machine Intelligence, IEEE Transactions on*, 30(2):328–341, 2008.

[22] H. Hirschmuller. Semi-global matching - Motivation, developments and applications. *Photogrammetric Week*, pages 173–184, 2011.

[23] H. Hirschmüller and D. Scharstein. Evaluation of cost functions for stereo matching. In *Computer Vision and Pattern Recognition, 2007. CVPR'07. IEEE Conference on*, pages 1–8. IEEE, 2007.

[24] A. Hosni, C. Rhemann, M. Bleyer, and M. Gelautz. Temporally consistent disparity and optical flow via efficient spatio-temporal filtering. In *Advances in Image and Video Technology*, pages 165–177. Springer, 2012.

[25] X. Hou and L. Zhang. Saliency detection: A spectral residual approach. In *Computer Vision and Pattern Recognition, 2007. CVPR'07. IEEE Conference on*, pages 1–8. IEEE, 2007.

[26] P.-J. Käck. Robust stereo correspondence using graph cuts. *Master's thesis, Royal Institute of Technology*, 2004.

[27] T. Kanade, H. Kano, S. Kimura, A. Yoshida, and K. Oda. Development of a video-rate stereo machine. In *Intelligent Robots and Systems 95.'Human Robot Interaction and Cooperative Robots', Proceedings. 1995 IEEE/RSJ International Conference on*, volume 3, pages 95–100. IEEE, 1995.

[28] R. Khoshabeh, S. H. Chan, and T. Q. Nguy. Spatio-temporal consistency in video disparity estimation. In *Acoustics, Speech and Signal Processing (ICASSP), 2011 IEEE International Conference on*, pages 885–888. IEEE, 2011.

[29] V. Kolmogorov. Convergent tree-reweighted message passing for energy minimization. *Pattern Analysis and Machine Intelligence, IEEE Transactions on*, 28(10):1568–1583, 2006.

[30] V. Kolmogorov and R. Zabin. What energy functions can be minimized via graph cuts? *Pattern Analysis and Machine Intelligence, IEEE Transactions on*, 26(2):147–159, 2004.

[31] D. Kondermann, R. Nair, S. Meister, W. Mischler, B. Güssefeld, K. Honauer, S. Hofmann, C. Brenner, and B. Jähne. Stereo ground truth with error bars. In *Computer Vision–ACCV 2014*, pages 595–610. Springer, 2015.

[32] L. Lucas, C. Loscos, and Y. Remion. *3D Video: From Capture to Diffusion*. John Wiley & Sons, 2013.

[33] D. Marr and T. Poggio. Cooperative computation of stereo disparity. *Science*, 194(4262):283–287, 1976.

[34] S. Martull, M. Peris, and K. Fukui. Realistic CG stereo image dataset with ground truth disparity maps. In *ICPR workshop TrakMark2012*, volume 111, pages 117–118, 2012.

[35] M. Menze and A. Geiger. Object scene flow for autonomous vehicles. In *Proceedings of the IEEE Conference on Computer Vision and Pattern Recognition*, pages 3061–3070, 2015.

[36] D. Min, S. Choi, J. Lu, B. Ham, K. Sohn, and M. N. Do. Fast global image smoothing based on weighted least squares. *Image Processing, IEEE Transactions on*, 23(12):5638–5653, 2014.

[37] B. A. Olshausen et al. Emergence of simple-cell receptive field properties by learning a sparse code for natural images. *Nature*, 381(6583):607–609, 1996.

[38] I. E. Richardson. *H. 264 and MPEG-4 video compression: Video coding for next-generation multimedia*. John Wiley & Sons, 2004.

[39] C. Richardt, D. Orr, I. Davies, A. Criminisi, and N. A. Dodgson. Real-time spatiotemporal stereo matching using the dual-cross-bilateral grid. In *Computer Vision–ECCV 2010*, pages 510–523. Springer, 2010.

[40] D. Scharstein and R. Szeliski. A taxonomy and evaluation of dense two-frame stereo correspondence algorithms. *International journal of computer vision*, 47(1-3):7–42, 2002.

[41] D. Scharstein, H. Hirschmüller, Y. Kitajima, G. Krathwohl, N. Nešić, X. Wang, and P. Westling. High-resolution stereo datasets with subpixel-accurate ground truth. In *Pattern Recognition*, pages 31–42. Springer, 2014.

[42] P. Shirley, M. Ashikhmin, and S. Marschner. *Fundamentals of computer graphics*. CRC Press, 2009.

[43] R. Szeliski, R. Zabih, D. Scharstein, O. Veksler, V. Kolmogorov, A. Agarwala, M. Tappen, and C. Rother. A comparative study of energy minimization methods for markov random fields with smoothness-based priors. *Pattern Analysis and Machine Intelligence, IEEE Transactions on*, 30(6):1068–1080, 2008.

[44] R. Tamassia. *Handbook of graph drawing and visualization*. CRC press, 2013.

[45] M. F. Tappen and W. T. Freeman. Comparison of graph cuts with belief propagation for stereo, using identical MRF parameters. In *Computer Vision, 2003. Proceedings. Ninth IEEE International Conference on*, pages 900–906. IEEE, 2003.

[46] P. Viola and W. M. Wells III. Alignment by maximization of mutual information. *International journal of computer vision*, 24(2):137–154, 1997.

[47] M. J. Wainwright, T. S. Jaakkola, and A. S. Willsky. MAP estimation via agreement on trees: message-passing and linear programming. *Information Theory, IEEE Transactions on*, 51(11):3697–3717, 2005.

[48] B. Wang and P. Dudek. A fast self-tuning background subtraction algorithm. In *Proceedings of the IEEE Conference on Computer Vision and Pattern Recognition Workshops*, pages 395–398, 2014.

[49] S. Wanner and B. Goldluecke. Reconstructing reflective and transparent surfaces from epipolar plane images. In *Pattern Recognition*, pages 1–10. Springer, 2013.

[50] J. S. Yedidia, W. T. Freeman, and Y. Weiss. Understanding belief propagation and its generalizations. *Exploring artificial intelligence in the new millennium*, 8:236–239, 2003.

Declaration of Honour

Hiermit versichere ich, dass diese Arbeit von mir persönlich verfasst wurde und dass ich keinerlei fremde Hilfe in Anspruch genommen habe. Ebenso versichere ich, dass diese Arbeit oder Teile daraus weder von mir selbst noch von anderen als Leistungsnachweise andernorts eingereicht wurden. Wörtliche oder sinngemäße Übernahmen aus anderen Schriften und Veröffentlichungen in gedruckter oder elektronischer Form sind gekennzeichnet. Sämtliche Sekundärliteratur und sonstige Quellen sind nachgewiesen und in der Bibliographie aufgeführt. Das Gleiche gilt für graphische Darstellungen und Bilder sowie für alle Internet-Quellen. Ich bin ferner damit einverstanden, dass meine Arbeit zum Zwecke eines Plagiatsabgleichs in elektronischer Form anonymisiert versendet und gespeichert werden kann.

Mannheim, Mai 2016

Ben John

Abtretungserklärung

Hinsichtlich meiner Abschlussarbeit mit dem Titel *„Comparison of Disparity Algorithms for Stereoscopic Video“* räume ich der Universität Mannheim/Lehrstuhl für Praktische Informatik IV, Prof. Dr. Wolfgang Effelsberg, umfassende, ausschließliche unbefristete und unbeschränkte Nutzungsrechte an den entstandenen Arbeitsergebnissen ein. Die Abtretung umfasst das Recht auf Nutzung der Arbeitsergebnisse in Forschung und Lehre, das Recht der Vervielfältigung, Verbreitung und Übersetzung sowie das Recht zur Bearbeitung und Änderung inklusive Nutzung der dabei entstehenden Ergebnisse, sowie das Recht zur Weiterübertragung auf Dritte.

Solange von mir erstellte Ergebnisse in der ursprünglichen oder in überarbeiteter Form verwendet werden, werde ich nach Maßgabe des Urheberrechts als Co-Autor namentlich genannt. Eine gewerbliche Nutzung ist von dieser Abtretung nicht mit umfasst.

Mannheim, Mai 2016

Ben John